TUNABLE OPTICAL FREQUENCY COMB IN SEMICONDUCTOR MICRORESONATOR

MASTER OF SCIENCE IN

PHYSICS

Submitted by:

NAVPREET KAUR

Roll No. 301904011

Under the guidance of

DR. SOUMENDU JANA

SPMS,

THAPAR INSTITUTE OF ENGINEERING AND TECHNOLOGY, PATIALA

CERTIFICATE

I hereby certify that the work which is being presented in the thesis entitled **"Tunable Optical Frequency Comb in Semiconductor Microresonator"**, is my own work carried out for the partial fulfilment of the requirement for the award of degree of Masters of Science in Physics submitted in School of Physics and Materials Science at Thapar Institute of Engineering and Technology, Patiala (Punjab), is an authentic record of my own work carried out under the supervisor of **Dr. Soumendu Jana** and refer to another researcher's work which are duly listed in the reference section. The content of this thesis is the product of my own work and contains no material which to a substantial extent has been accepted for the award of any other degree of this or any other educational institute, except where due acknowledgement is made in the thesis.

(Navpreet Kaur)

Date: 30 July 2021. Roll no: 301904011

It is certify that the above statement made by the candidate is correct and true to the best of knowledge and belief.

Dr. Soumendu Jana
Supervisor
(Associate Professor)
School of Physics and Materials Science,
Thapar Institute of Engineering and Technology, Patiala

ACKNOWLEDGEMENT

Work shown in this thesis would not have been possible without the support of many people. It is a pleasure to convey my sincere gratitude and appreciation to all of them in my humble acknowledgement.

First, I would like to thank my supervisor **Dr. Soumendu Jana** for his guidance, help, inspiration and continuous support. Without his motivation and support this work would not have been successful. I have learnt how to approach a problem by systematic thinking. I sincerely thank him from my heart and really could not have imagined a better advisor and mentor than him for my thesis.

I wish to express my sincere thanks to **Dr. O.P. Panday,** Professor and Head, School of Physics and Material science, Thapar Institute of Engineering and Technology, Patiala for providing me all the necessary facilities for my research.

Besides my supervisor, I express my heart-felt gratitude to **Mr. Neeraj Sharma, Ms. Jaspreet Kaur, Mr. Vikas** and **Ms. Anjali Saini,** Research Scholars, who have always been there for me with their supporting hands whenever Ineeded them. Also thanks for sharing their valuable experience with me. I would not have been able to complete my thesis without their cooperation.

Finally, I would like to acknowledge the people who mean a lot to me, **my parents, grandparents** and younger **brothers** whose love, care and support gave me the strength to successfully complete my dissertation. I really want to thank them for their support, both financially and emotionally throughout my degree.

I also thank the almighty for giving me strength and patience to walk on the path of truth.

Navpreet kaur

CONTENTS

ABSTRACT

Optical frequency comb, a spectrum of equidistant lines, has attracted theoretical and experimental research interest since more than the last two decades. In this thesis work we theoretically generated the optical frequency comb in a dissipative microresonator based on a vertical cavity surface emitting laser (VCSEL). The vertical cavity surface emitting laser is coupled with a saturable absorber and frequency selective feedback. Optical frequency comb has been investigated for different input profiles namely Gaussian, super-Gaussian, sinh-Gaussian and cosh-Gaussian. Both chirped and unchirped profiles have been studied. In all cases optical frequency comb has been generated via cavity soliton formation of the input field. Split-step Fourier transformation based numerical method has been used to find the frequency comb. The generated optical frequency comb from different profiles are then compared. The parametric regions of optical frequency comb generation have been identified for each profile. The possibility of tuning the optical frequency comb has been highlighted.

CHAPTER 1

1.1 INTRODUCTION

Frequency comb is an interesting topic of contemporary research that has attracted renewed attention since the Nobel Prize was awarded to Roy J. Glauber, John L. Hall and Theodor W. Hansch in 2005 [1]. Optical frequency comb (OFC) is a spectrum consisting of equidistant lines. It measures a very high frequency of short pulses of light. It can be achieved by ultrafast lasers because they accurately measure the higher frequency [2]. For OFC if we make a graph of intensity corresponding to the frequency, the 'teeth' or line come with different colours; arranged according to their pulse with small frequency comes at left and the pulse with large frequency comes at right of the graph. OFCs give equally spaced frequency lines [3, 5]. They are creating novel applications for precision spectroscopy [6], sensing, microwave synthesis, optical waveform generation, and physical sciences [7,8]. Earlier, frequency comb has been generated using the mode-locked laser but unfortunately this leads to limited frequency pitch. It stabilizes the repetition rate and carrier envelope phase [9]. To produce the broadband frequency comb, femtosecond mode-locked lasers are a very suitable source. Its optical spectrum consists of equally spaced descreste lines to pulse repetition frequency ($frep$). Outside the laser cavity, if we use strong optical nonlinearities, for example from highly nonlinear optical fibers the comb can be further broadened [10]. We get the output in the time domain, but results in the time domain cannot be easily observed so we have to consider a fourier transformation which converts the time domain into frequency domain and stabilizes the carrier phase with respect to pulse envelope. Because the group and phase velocities are different in the laser cavity, so from pulse to pulse, this phase is not constant. The output of a mode-locked laser gives combs of frequencies that are separated by the repetition rate. In narrow bandwidth, pulses interfere, and we can find the signal only where they add constructively [11] i.e., have a phase shift of $2n\pi$.If the time between the pulse train is τ , these frequencies are $fn = n/\tau = n\,frep$, where n is integer and $frep = 1/\tau$ is the repetition frequency of pulse trains. If carrier phase is integer multiple of 2π, there is no offset, but if it is not integer multiple of 2π then there will be offset frequency i.e., $fn = n\,frep + \delta$

1.2 LITERATURE REVIEW:

Little more than 20 years ago, frequency combs were found as a laser technology which can count the fast oscillating cycles of light [14]. As mentioned earlier, the frequency comb is a spectrum which consists of equally spaced lines i.e., having equally spaced frequency components [15,16]. This shows the optical spectrum and there are millions of little teeth of optical comb. OFC was found to count the cycles from optical atomic clocks [12]. OFC

attracts attention because of many applications for example frequency metrology, precision spectroscopy, distance measurement or telecommunication. Frequency comb can be produced in many ways like mode-locked laser, four wave mixing, saturable absorber etc. However, the size of mode locked lasers tells that these systems would never be available widely and they have limited capabilities [13]. To solve this problem, there was new development to control the spectrum of mode-locked lasers, which leads to optical frequency comb. The self-referencing technique helped the frequencies of combs to be “locked” to radio frequency [17,18,19,20]. The Fourier transform gives the equally spaced lines of OFC in the frequency domain [21,22]. Virtually, everything in this world may be described by the waveform which is defined as a function of time or space [23]. Frequency transform gives a good way of viewing these waveforms [24]. OFC was found to support the most precise atomic clocks. Optical clocks are based on atom’s optical transitions that operate on high frequency as compared to the microwave atomic clocks. This is used to define the second with high accuracy. Applications of OFC have expanded and there are many developments in this technology. Between the comb lines of frequency combs, frequency stability and phase coherence can provide good merits. Mode-locked lasers can produce frequency comb that allow optical frequency metrology to extend in the 1.55μm region. OFC can be shown in different ways. Among all these, we use VCSEL to generate the frequency combs. VCSEL has many advantages over other lasers like low power consumption [27], use of a low current to operate (under 10mA) and gives an array of output beams[28, 29]. The gain switching method starts to generate the OFC [30, 31]. We didn't get the equal frequency separation in the mode-locked laser but with the help of gain switching, we can equally maintain the frequency separation [32, 33].

1.3 MOTIVATION

Although a lot of work has been done on OFC during the last two decades till several issues related to OFC are unanswered. For example, tunability of OFC, role of various saturable absorbers etc. need more research attention. Frequency combs have been studied in microresonators in recent times. It would be a very novel idea to investigate the frequency comb generation in the light of cavity soliton. Therefore, our present investigation will try to club the concept of cavity soliton in frequency comb generation.

1.4 OBJECTIVE

In view of gap in present scientific literature, we purpose to investigate

1. the generation of optical frequency comb using cavity solitons in microcavity.
2. to identify the role of writing beam profiles in the generation of optical frequency comb.

1.5 METHODOLOGY

We generate OFC in a microresonator that comprises VCSEL with a saturable absorber (SA) and coupled with frequency selective feedback (FSF). The governing equation for the electric field of the electromagnetic field inside the microresonator can be expressed by the Complex Ginzburg-Landau equation (CGLE). The following Complex CGLE can be used to express the cavity field of our microresonator system.

$$\frac{\partial E}{\partial t}=[-\ (1\ -\ i\theta)\ +\ \frac{\mu(1-i\alpha)}{1+|E|^2}-\ \frac{\gamma(1-i\beta)}{1+s|E|^2}+\ i\Delta]\ E\ +\ (a\ -\ ib)E \qquad \text{.....(1)}$$

where, E is the slowly varying amplitude of the electric field. θis the cavity mistuning parameter, i.e., it captures the mismatch in frequency between the cavity field and the external field. The cavity loss is so normalized that it leads to the "1" in the first term in the right hand side of the equation. α and β are line width enhancement factors for active and passive material respectively. μ and γ are pump parameters for active and passive parameters respectively. Δ is the transverse laplacian. The last term is the FSF term that compensates for the loss of the cavity and helps in stabilizing the cavity soliton, via which we generate OFC. a and b are the feedback parameters.

The aforesaid CGLE, i.e., the governing equation generally does not have an closed form exact analytic solution. However, some analytical-numerical methods, e.g., separation method (splitting the CGLE into two eigenvalue problems and solving) by Firth et.al. can give an essential idea of the solution zone [34]. One can try to solve the CGLE by an approximate analytical method (eg: vibrational method) as done by B. Kaur et.al [35]. For the current investigation, following the footsteps of the leading researchers, we adopt a numerical method, namely, split step fourier method to generate OFC by solving this governing CGLE. In general, numerical methods of two major categories are used to solve such CGLE or similar perturbed nonlinear Schrodinger equations: (1) finite difference time domain (FDTD) method and (2) Split-Step Fourier transform method (SSFM). We choose a direct numerical path and prefer SSFM over FDTD as the former is the faster routine and suffers from less instability. [55]. SSFM is a pseudo-spectral method and is faster than general numerical methods up to an order of magnitude to achieve the same accuracy.

1.5.1 SPLIT- STEP FOURIER METHOD

It is a pseudo-spectral numerical method used to solve the nonlinear partial differential equation like the nonlinear Schrodinger equation and different CGLE (as one we used in our investigation). This method is used to find the solution in small steps and treat the linear and nonlinear steps separately. This method is used in the field in which light propagates along a waveguide or the optical field evolves with time, but the linear and nonlinear interaction make it difficult to find the solution. In this method the length of the waveguide or the evolution time is split into small steps/ segments. The input field is then rewritten into Fourier domain. Now the effect of propagation (diffraction, dispersion etc.) is incorporated

into the problem and then integrated. The result, i.e., the field at the end of the small segment is then written using the inverse Fourier transform. Nonlinearity is introduced in an interesting manner. First the average of the nonlinearity is calculated and then is added in the half-way of the segments. Also, there are other variants of the method. A general description of the steps are portrayed below.

Firstly, the governing equation (here, the CGLE) is rewritten in operator form as

$$\frac{\partial E}{\partial z} = (D + N)E. \qquad \text{..... (2)}$$

Where D is differential operator that accounts for dispersion and absorption in a linear medium and N is a non-linear operator. The SSFM obtains appropriate solutions by assuming that in propagating the optical field over a small distance h, the dispersive and nonlinear effects can be pretended to act independently. Propagation from z to $(z + h)$ is carried out in two steps. In the first step, nonlinearity acts alone, and $D = 0$. In the second step, dispersion acts alone, and $N = 0$. Mathematically,

$$E(z + h, T) \approx exp(hD)exp(hN)\ E(z, T). \qquad \text{..... (3)}$$

The exponential operator can be evaluated in the Fourier domain using the prescription

$$exp(hD)B(z, T) = F^{-1}exp[hD(i\omega)]F\ B(z, T). \qquad \text{..... (4)}$$

Where F denotes Fourier transform operator.

To estimate the accuracy of the split step Fourier method, we note that a formally exact solution of equation (1) is given by

$$E\ (z + h, T) = exp[h(D + N)]\ E(z, T). \qquad \text{..... (5)}$$

If N is assumed to be z independent. At this point, it is useful to recall the Baker-Hausdorff formula [14] for two non-commuting operators a and b.

$$exp(a)exp(b) = exp(a + b + \frac{1}{2}[a, b] + \frac{1}{12}[a - b, [a, b]] + \ldots) \qquad \text{..... (6)}$$

where, by using eqn. (6) with $a = hD$ and $b = hN$, the dominant error term is found to result from the single commutator . Thus the split-step Fourier method is accurate to second order in the step size h.

CHAPTER 2

In this chapter we describe the OFC in detail. We also discuss the components and concepts associated with the formation of OFC in our investigation.

Scientists used the laser that gives continuous and closely spaced pulses that have many different colours [36]. Time and frequencies are inversely related i.e. if time is small it results in larger frequency numbers. Let we have light of four colours i.e., blue, red, green and yellow [37]. Blue light moves faster than the red light and green and yellow moves between them. If we make a graph corresponding to the frequency comb, we get the line that comes with different colours and they are arranged according to their oscillation. Blue light rotates fast but the red light rotates slowly. If blue takes four rotations then red takes only one rotation or oscillation at that time [38] that means pulse oscillates very slowly, comes at left i.e. red and the pulse that oscillates very fast comes at right of the graph. The graph is between intensity (X-axis) and frequency (Y-axis).

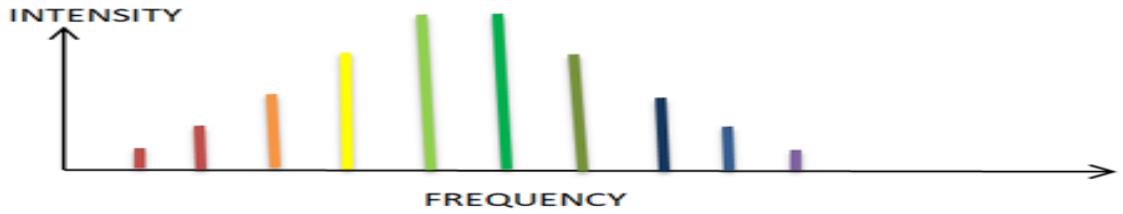

Figure 2.1.1: OFC having equally spaced frequency components

A.TIME DOMAIN

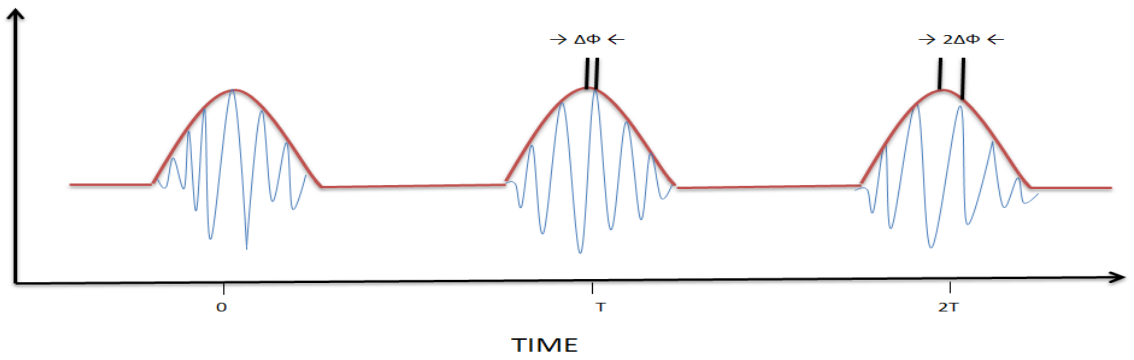

B. FREQUENCY DOMAIN

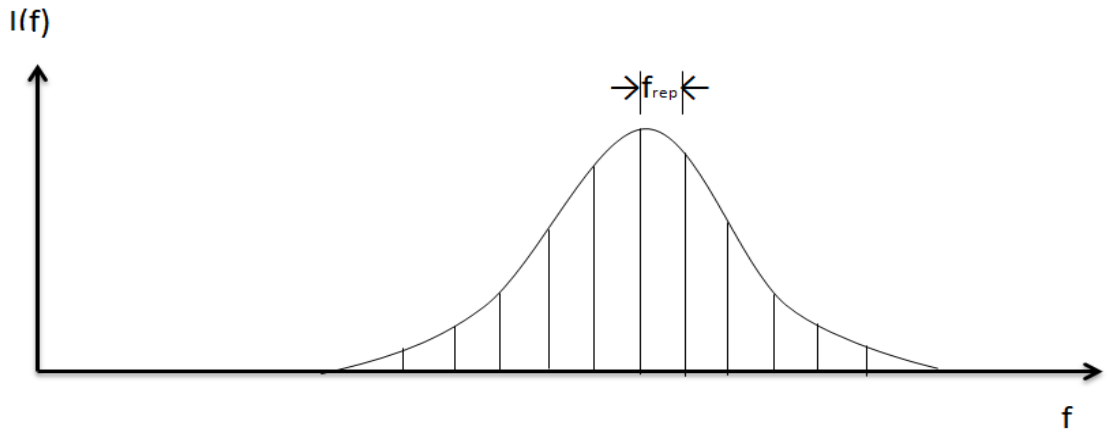

Figure 2.1.2 :(A) In the time domain, the phase between the carrier (blue) and the envelope (red) evolve from pulse to pulse by the amount $\Delta\phi$.
(B) In the frequency domain, the elements of the frequency comb of a mode-locked pulsetrain are spaced by frep.

Teeth are closely and equally spaced and are used to measure the light emitted by the laser. If the pulse is fast then it takes a small time and frequency becomes high [39]. Scientist used 'mode-locked' which emits femtosecond (10^{-15}sec) pulses that have millions of seconds that result in several hundred thousand frequencies or teeth [40].

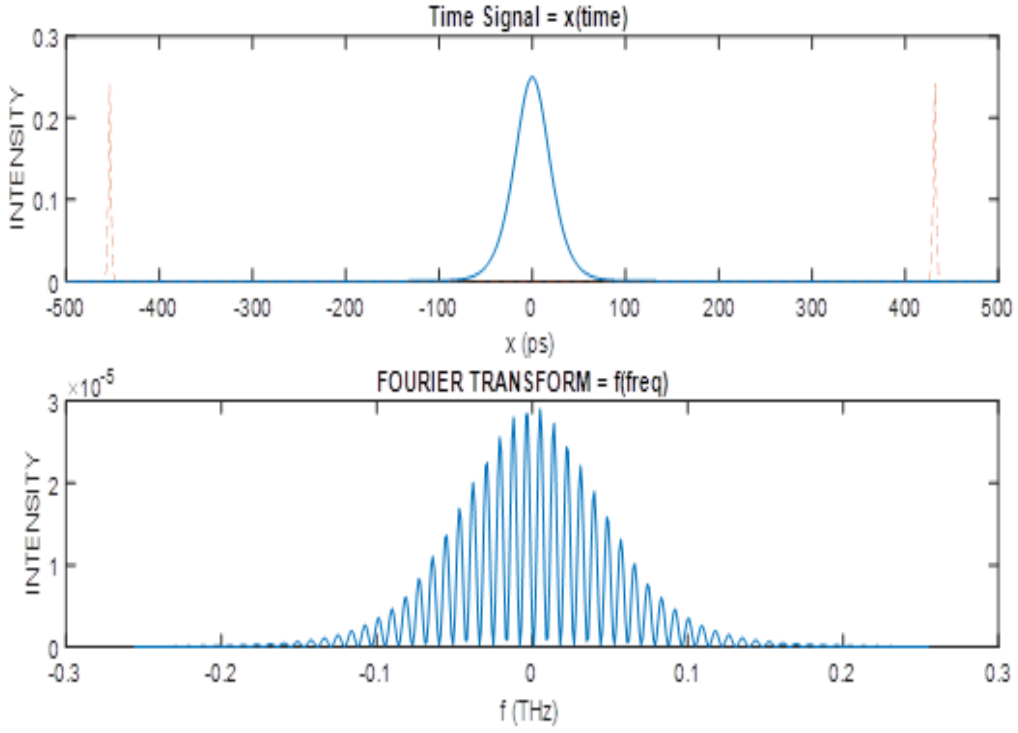

Figure 2.1.3: The injected signal (upper panel) and the generated optical frequency comb (lower panel). The system parameters are $\theta = 1.0$, $\mu = 1.34$, $\alpha = 2.4$, $\gamma = 0.42$, $\beta = 0$, $s = 10$, $\lambda = 0.42$, $\sigma = 0.316$, $\omega = 1.7$

In the upper panel of the above figure, the beam is given as input (in solid blue) which is divided into two spikes (in dotted red). The spikes are at the same distance from the beam. These spikes are thin that's why frequency comb in output will be wide, which is in space [41]. In all other lasers, light reflects in the mirror cavity repeatedly but in 'mode-locked' lasers, peaks of different colours coincide at regular intervals. Spacing between the lines of the frequency combs can be determined by Time between pulses. As fast as the repetition of pulses, the space will be less between the teeth [42].

To know about the mechanism of OFC formation in our method we need to learn about saturable absorber, soliton, cavity soliton and VCSEL. We have a saturable absorber in VCSEL which will help in achieving a cavity soliton (a unique family of localized optical structure/ spot inside the VCSEL cavity) as well as mode-locked. The OFC is investigated for such cavity solitons.

2.2 COMPONENTS OF GENERATION OF OFC

There are many methods to produce OFC like mode-locking, four wave mixing etc. We generate via cavity soliton, which is based on the microcavity of a VCSEL. The components to produce the optical frequency are described below.

2.2.1 CAVITY SOLITON:

Solitons are wave packets that maintain their shape and size during the propagation and even after collision with another one [47]. Conservative soliton will create if two phenomena balance each other i.e. dispersion, or self diffraction induced broadening is balanced by nonlinearity induced self-phase modulation or self-focusing. Conservative systems are rare and so the conservative soliton [48]. A dissipative soliton can be created in a lossy system, when the balancing condition for corservative soliton is present and additionally and essentially the loss of the system is balanced by an external gain [43]. Cavity solitons (CS) are a unique class dissipative soliton that can be generated inside a cavity of a wide cross sectional area resonator. CSs are bright peaks over a dark homogeneous background [44, 45]. They are created below threshold and the whole system is mathematically bistable. Soliton can't be stable if the system has any loss so this loss is compensated by the gain. We gave the holding beam to get gain in the system. Now, we have two other methods by which the system can gain i.e., frequency selective feedback and saturable absorber. In optical cavities, these are bright spots of light. The cavity contains a nonlinear medium that provides the confinement of the light [46].

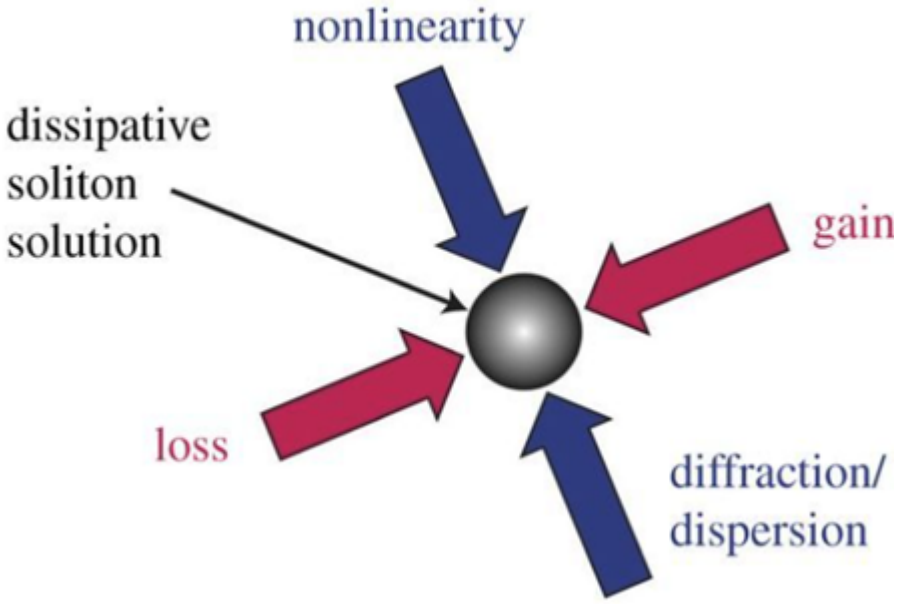

Figure2.2.1: Continuous and discrete solution in conservative and dissipative system.

2.2.2 VERTICAL CAVITY SURFACE EMITTING LASER , CS and OFC

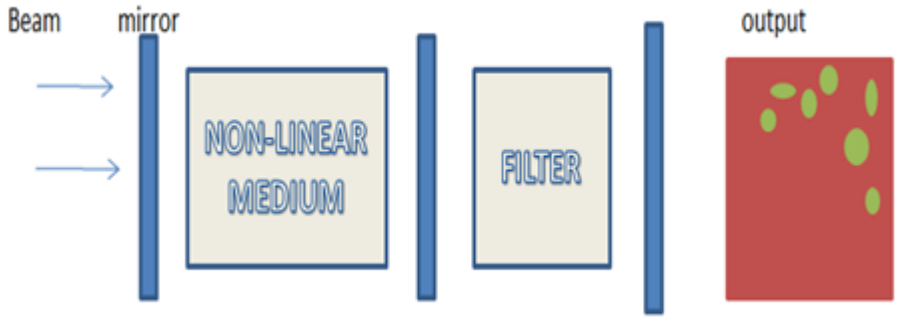

Figure 2.2.2: Structure of vertical cavity surface emitting laser (VCSEL).

We can produce the OFC by using many different ways, but in this thesis we use the idea of soliton for the generation of the OFC, particularly cavity soliton. We take two mirrors, one is partially reflecting i.e 90% and the other is full reflecting i.e 100% and the active region is on the first mirror stack and a second mirror stack is on the active region [52]. Now put the saturable absorber in it [51]. Cavity soliton needs to be bistable. First, we will incident a beam on it which creates a non-linearity in the system. The laser beam, that was diffracting,

is now trying to focus because of this non-linearity in the material. There is a loss in the system because of the saturable absorber so to overcome this we have a feed-back system. When the loss, gain, self-diffraction and self-focusing will balance then we will get a spot which is called soliton. We create OFC in time domain i.e., temporal cavity soliton and it should be thin so that we can get a wider OFC. If we have a cavity soliton in the time domain then take the Fourier transformation and then we get the OFC. The thinner the cavity soliton, the OFC will be wider. If peaks are nearer, the frequency comb of the first will interfere with the other one and that's why we get the wider OFC. We can also erase this bright spot by giving $180°$ opposite phases of the pulse that we gave. We can't make it too close because this will oppose the formation of other soliton but beyond some distance, they can be created anywhere. If we put this cavity soliton in the frequency domain then we will get the optical frequency spectrum, whose structure is almost like a 'comb' or 'tooth'. Frequency is equally spaced here, because there is phase change in the cavity [53]. VCSEL are the type of laser diode that offer some important properties because of their ability to emit the light vertically and in perpendicular direction to their semiconductor layers. These are cost effective devices, small in size and easy to use and with a high modulation bandwidth.

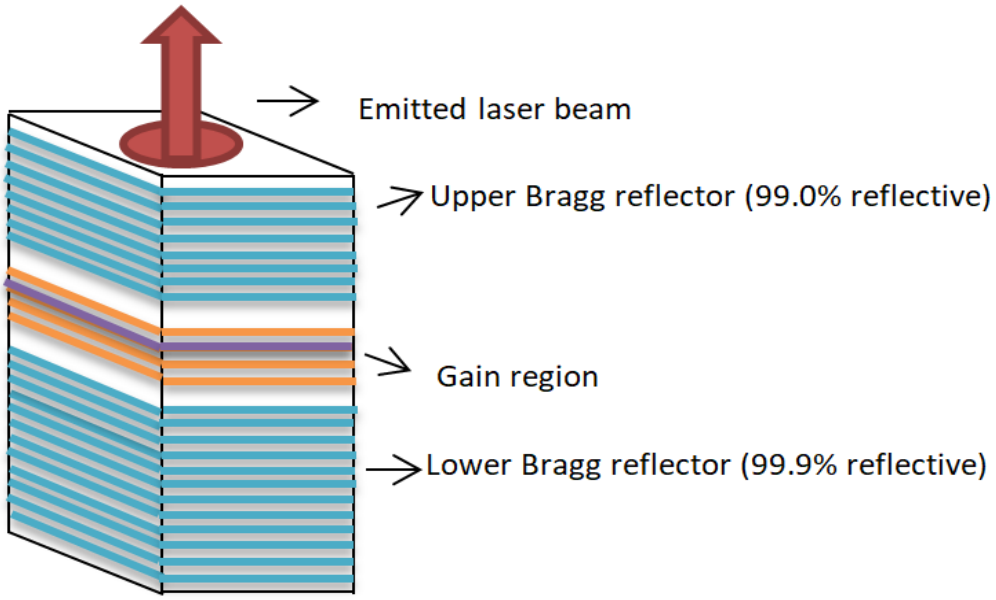

Figure 2.2.3: Structure of VCSEL emitting the light in the perpendicular direction to the chip surface.

VCSELs are the laser diodes, where the light emits in the perpendicular direction to the surface. Between these we have the active region and its thickness is a few micrometers. In many cases, the active region produces output in the range $0.5 - 5mW$ by electrically pumping. VCSELs emit wavelengths mostly in the range of $750 - 980nm$. Long wavelength, example- $1.3\mu m$, $1.55\mu m$ or even beyond $2\mu m$ can be obtained with dilute nitrides and from the device based on indium phosphide. Optical amplifiers are also there and are similar to VCSEL. Basically, they are VCSELs with less top mirror reflectivity. An important practical advantage of VCSELs as compared to edge emitting semiconductor laser,

is that they can be tested and characterized directly after growth i.e., before the wafers are cleaved. Special VCSELs are developed which are essentially thresholdless lasers. They are interesting in this domain because they allow the utilization of quantum effects related to the modification of the mode density by the cavity. With such technique, a threshold current of only $36\mu A$ has been demonstrated. Much higher powers can be generated with a VCSEL array. In comparison with conventional edge-emitting laser diodes, VCSEL arrays have low power conversion efficiency, but these have merits for applications like simplification of beam shaping optics, the small emission linewidth, the higher wavelength stability etc.

CHAPTER 3

3.1 RESULTS AND DISCUSSION

In this chapter we present our result to generate OFC in a microresonator cavity that comprises a VCSEL with SA and coupled with FSF. We use different input field pulse profiles to create CS in the microcavity. The input field profiles, corresponding cavity soliton and OFC are described below. Also, the parametric region of CS and hence OFC formation is mentioned in the corresponding tables.

1. For GAUSSIAN profile:

Gaussian profile is given by

$$U(0,T) = U_0\, exp\left(-\frac{T^2}{2{T_0}^2}\right),$$

Where $U_0$is maximum amplitude T is time and T_0 is pulse width .

(a) (b)

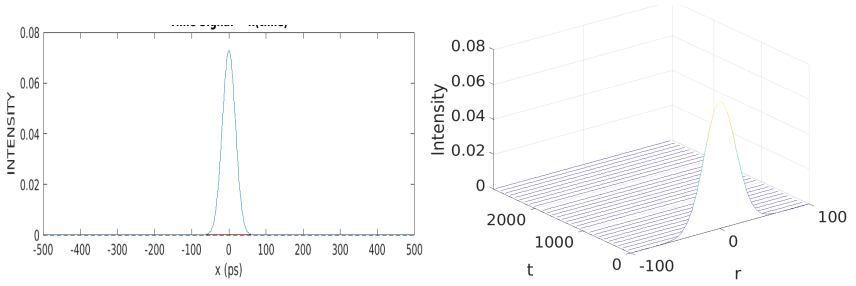

(c)

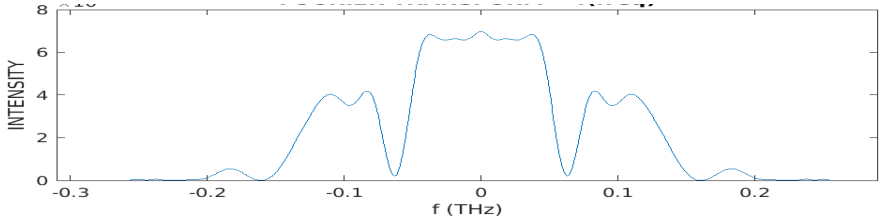

Figure 3.1.1: (a) Blue line is the initial pulse which is in the time domain (b) 3D profile for the same. (c) Shows the output in the frequency domain. Here $\alpha = 2.7$, $\beta = 0.5$, $\gamma = 0.5$, $s = 10$, $\lambda = 0.5$, $\sigma = 0.3$, $\omega = 1.6$, $\theta = 1.3$.

The Figure 3.1.1: (c) suggests that we didn't get a good quality OFC here for the given value of parameters. Now, if we change the parameter $\alpha = 10.1$, we can observe the OFC given below.

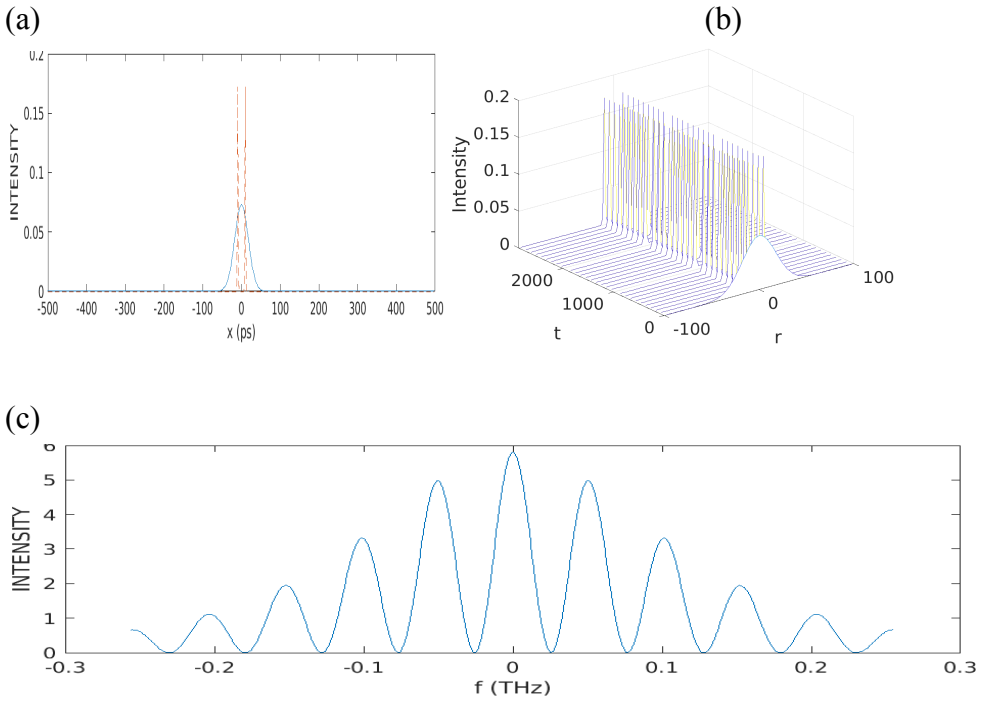

Figure 3.1.2: Initial and final pulse profile and corresponding frequency comb (a) The blue line is the initial pulse and narrow cavity soliton represented by a dotted red line. Initial pulse splits into two cavity solitons of high intensity (b) 3D profile of initial pulse (c) The corresponding OFC. Here $\alpha = 10.1$and the rest of the parameters are the same as in figure 3.1.1(c).

The generation of exact frequency comb is slightly difficult, but we check it by varying the different parameters. The range in which we found the OFC for gaussian pulse is given below.

TABEL-1: Parametric values / range for acceptable OFC for Gaussian profile

parameters	value/range	parameters	value/range
α	10.11 to 10.12	λ	0.49999 and 0.511
β	5 to 5.91	σ	0.3 and 0.299

γ	0.4,0.5,0.515,0.516 and 0.7	ω	1.61 to 1.67
s	9.9 to 10.1,10.11,10.12 and 10.21	θ	1.3 to 1.36

If we introduce the chirping in the Gaussian profile, the chirped Gaussian pulse is given by:

$$U(0,T) = U_0\, exp\left(-\frac{(1+iC)T^2}{2{T_0}^2}\right)$$

For $c = 1$, we don't get OFC

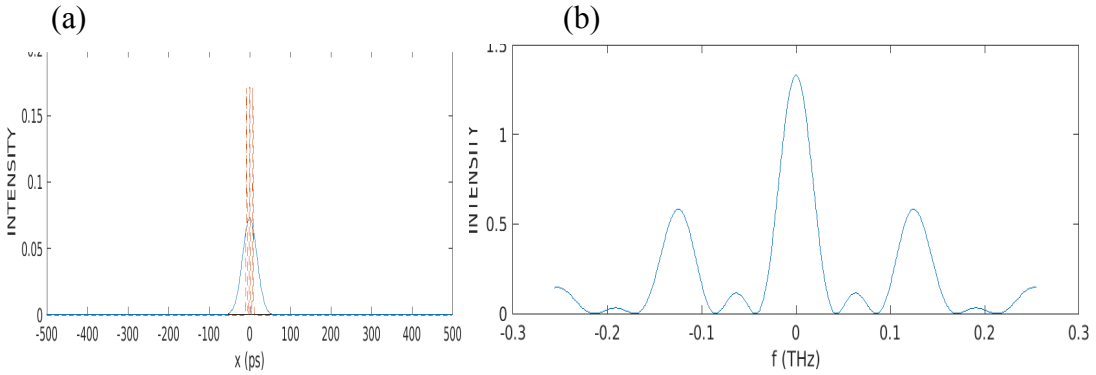

Figure 3.1.3: (a) and (b) Shows the initial and final pulse profile and corresponding frequency comb but it is not an exact OFC. here all the parameters are same as in figure 3.1.2(c)

Now if change some parameters like $\beta = 0.7$, we get the OFC

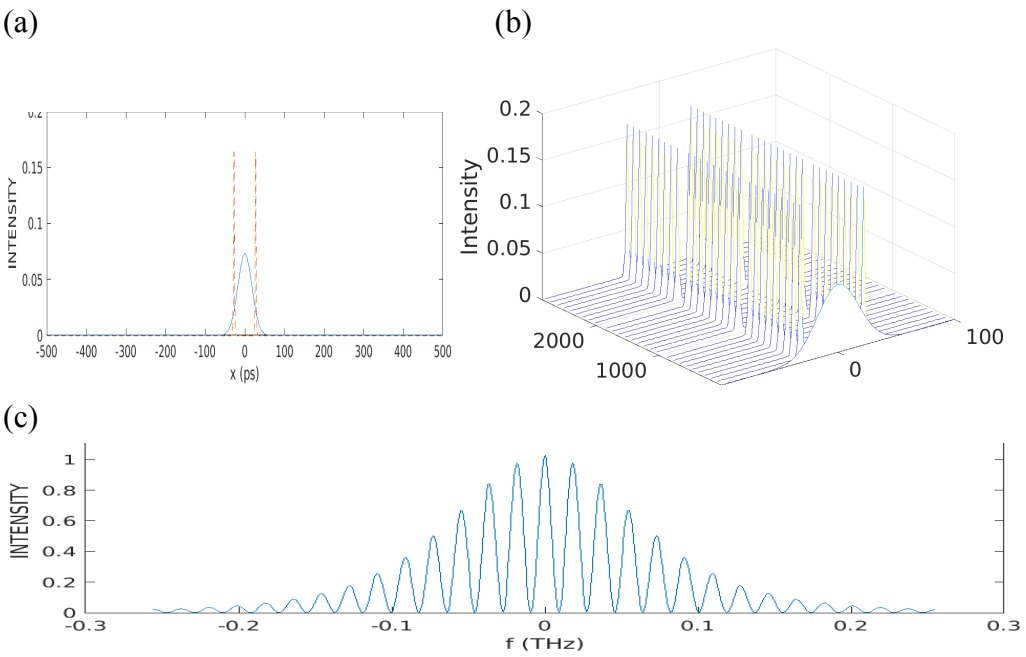

Figure 3.1.4: (a) Initial pulse with blue line splits into two cavity soliton with dotted red lines. (b) 3D spectrum of figure 3.1.4(a). (c) Shows the frequency comb. Here $\beta = 0.7$and the rest of the parameters are the same as in figure 3.1.3(c).

TABLE-2: Range in which we found the frequency comb for Chirping Gaussian pulse where $c = 1$ is given below.

parameters	value/range	parameters	value/range
α	0.5999	σ	0.3,0.31
β	0.5,0.7,0.9	ω	1.6,1.7
s	10	θ	1.3 to 25
λ	0.5		

If we introduce $c = 2$, we don't get the OFC

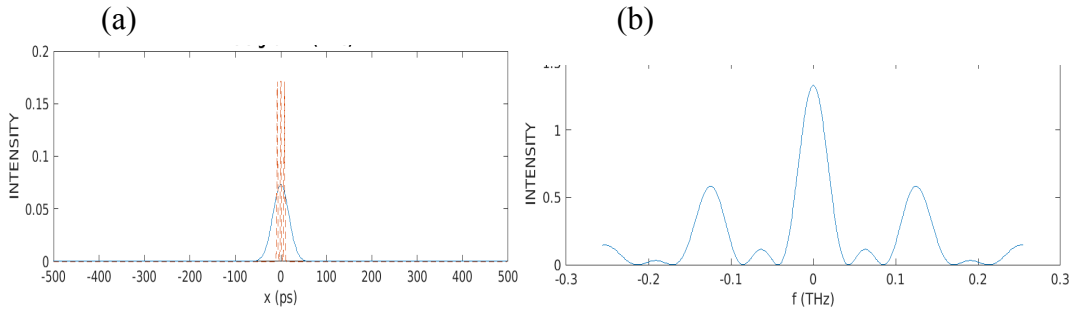

Figure 3.1.5: (a) Initial pulse in time domain. (b) Shows the generation of OFC, but it is not exact. all parameters are the same as in figure 3.1.2(c).

To get OFC for chirping $c = 2$ we have to change the parameter $\alpha = 6$, we will get the OFC.

(a) (b)

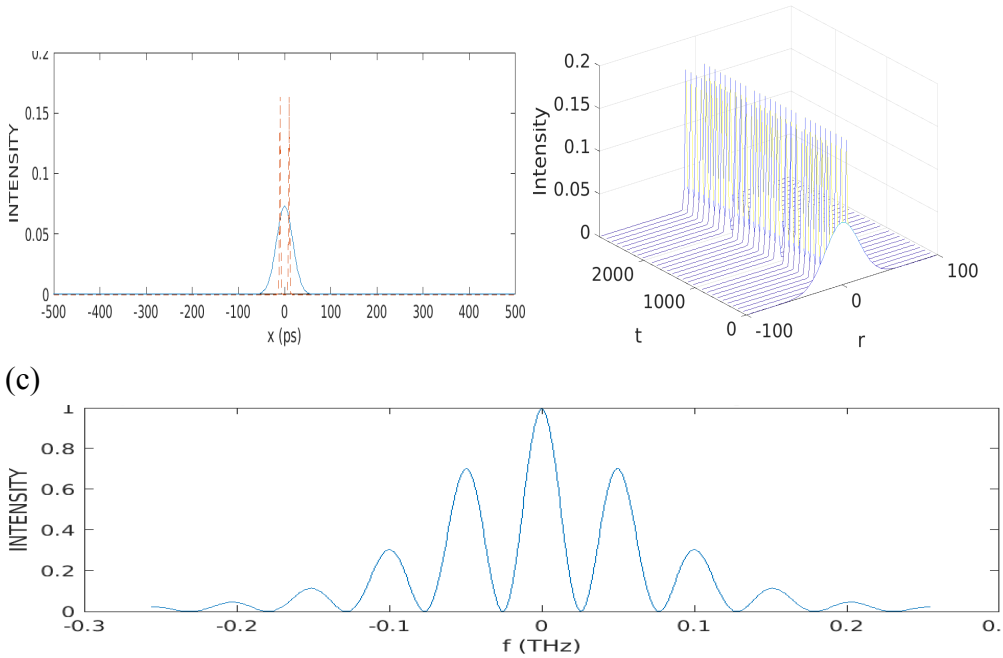

Figure 3.1.6: (a) Blue line is the initial pulse split into two cavity soliton. (b) 3D profile for the figure 3.1.6(a). (c) Corresponding OFC. here $\alpha = 6$and the rest of the parameters are the same as in figure 3.1.5(c).

TABLE-3: Range in which we found the frequency comb for Chirping Gaussian where $c = 2$ is given below.

parameters	value/range	parameters	value/range
α	6 to 8	σ	0.3,0.31,0.33
β	0.5,0.9,1	ω	1.6,1.7
s	10	θ	1.3 to 30
λ	0.51,0.52		

If we introduce the value of $c = 3$, we don't get the OFC.

(a) (b)

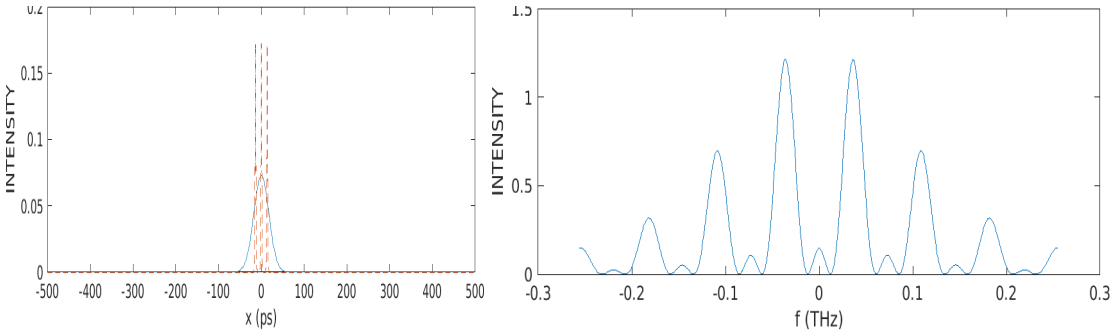

Figure 3.1.7: (a) Initial and final pulse profile time domain. (b) Shows the corresponding OFC, but not perfect OFC. Here all the parameters are the same as in the figure 3.1.2(c).

If we change the parameter $\lambda = 0.51$, we will get the frequency comb.

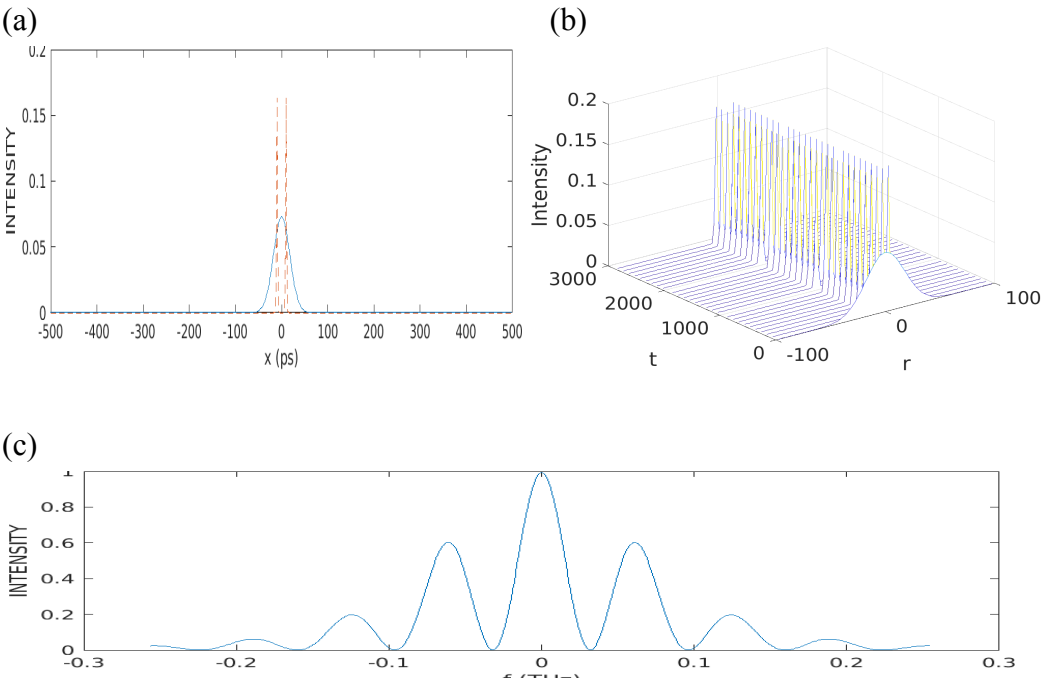

Figure 3.1.8: (a) Initial pulse in time domain splits into two soliton. (b) 3D profile for initial pulse. (c) Shows the frequency comb. Here $\lambda = 0.51$and the rest of the parameters are the same as in figure 3.1.2(c).

TABLE-4: Range in which we found the frequency comb for chirping gaussian where $c = 3$ is given below.

parameters	value/range	parameters	value/range
α	7,8	σ	0.3,0.31,0.32

β	0.5,0.8,0.9,1 and 2	ω	1.6,1.61 to 1.63
s	10,10.1	θ	1.3 to 30
λ	0.5,0.51,0.52		

2. For SUPER GAUSSIAN profile:

The super-Gaussian profile is given by

$$U(0,T) = U_0\, exp\left[-\left(\frac{T}{T_0}\right)^{2n}\right],$$

where U_0 is maximum amplitude T is time, T_0 is half width.

When $n = 1$, it becomes a gaussian pulse. We varied from $n = 2\ to\ 4$.

For $n = 2$, keeping the parameters same and see the spectrum

(a) (b)

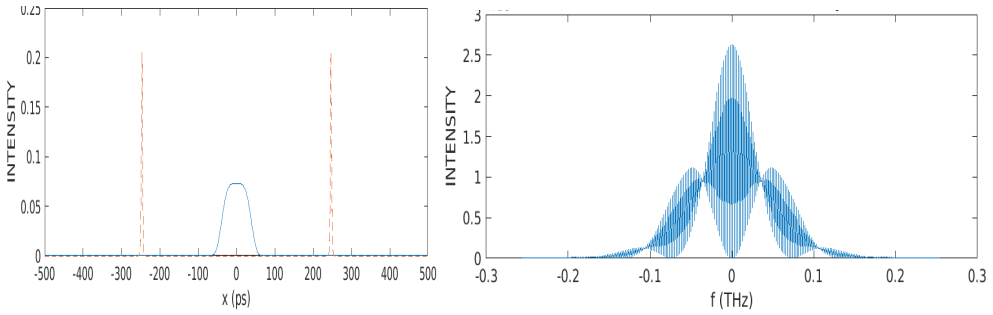

Figure 3.1.9: (a) Initial pulse is with blue line which is in the time domain and split into two cavity soliton which are in red dotted line. (b) Generation of frequency comb but not exact OFC. Here $\alpha = 2.7$, $\beta = 0.5$, $\gamma = 0.5$, $s = 10$, $\lambda = 0.5$, $\sigma = 0.3$, $\omega = 1.6$, $\theta = 1.3$.

In the above figure, we didn't get the OFC.

Now, To get the OFC for Super Gaussian Profile we have to change the parameter $\alpha = 2.8$ and we will get the OFC.

(a) (b)

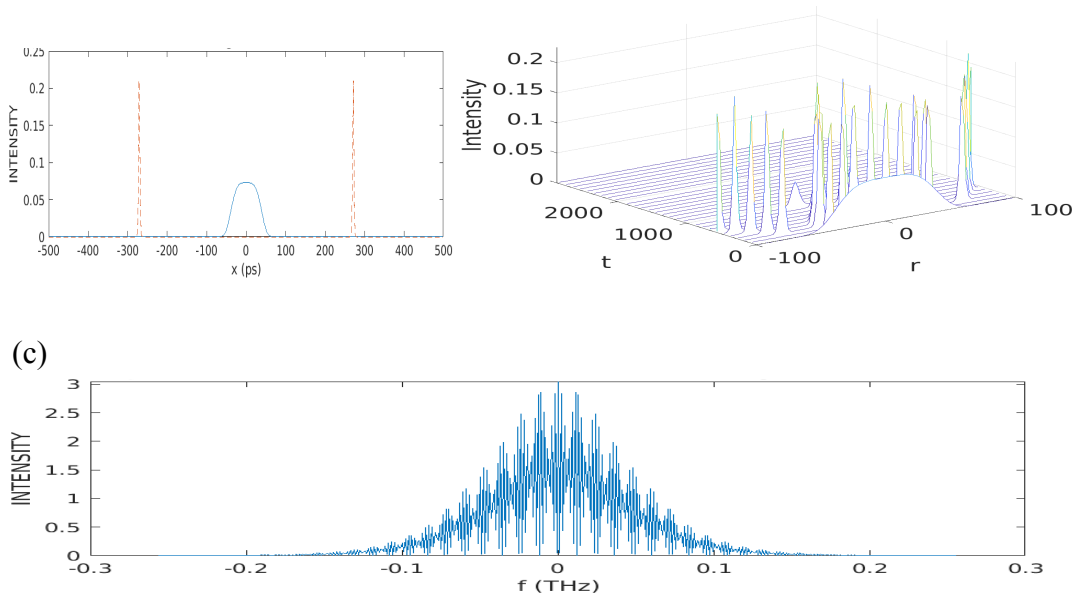

Figure 3.1.10: Initial and final pulse profile and corresponding frequency comb. (a) Blue line is the initial pulse which splits into two cavity solitons of high intensity denoted by red dotted lines. (b) Shows the initial pulse in 3D. (c) Frequency comb. Here $\alpha = 2.8$and the rest of the parameters are the same.

TABLE-5: Range where we can get the OFC for Super Gaussian pulse when parameters will change, is given below.

parameters	value/range	parameters	value/range
α	2.8 to 3	σ	0.3
β	0.48,0.5,0.53 to 0.59	ω	1.8,1.81,1.82,1.6,1.9 and1.91
s	9.8 to 10	θ	1.3 to 30
λ	0.47,0.5,0.51 and 0.52		

If we introduce the chirping in super gaussian pulse i.e.,

$$U(0,T) = U_0\, exp[-\frac{1+ic}{2}\left(\frac{T}{T_0}\right)^{2n}]$$

For $c = 1$, we get the OFC.

(a) (b)

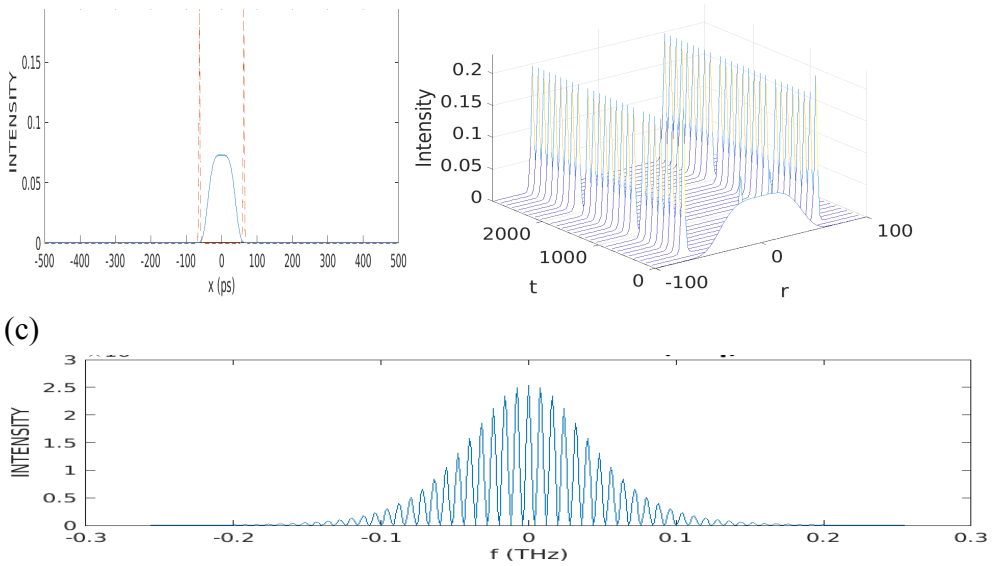

Figure 3.1.11: Initial and final pulse profile and corresponding frequency comb. (a) Blue line is the initial pulse which splits into two cavity solitons of high intensity denoted by red dotted lines. (b) Shows the initial pulse in 3D. (c) Corresponding frequency comb. Here all the parameters are same as in figure 3.1.10

TABLE-6: Range in which we observed the frequency comb for Super Gaussian pulse where $n = 2$ and $c = 1$.

parameters	value/range	parameters	value/range
α	3	σ	0.3,0.31
β	0.5,0.7,0.9	ω	1.6 to 1.8
s	10,10.1,10.3	θ	1.3 to 30
λ	0.5,0.6		

Similarly, If we introduce the chirping $c = 2$, we get the OFC.

(a) (b)

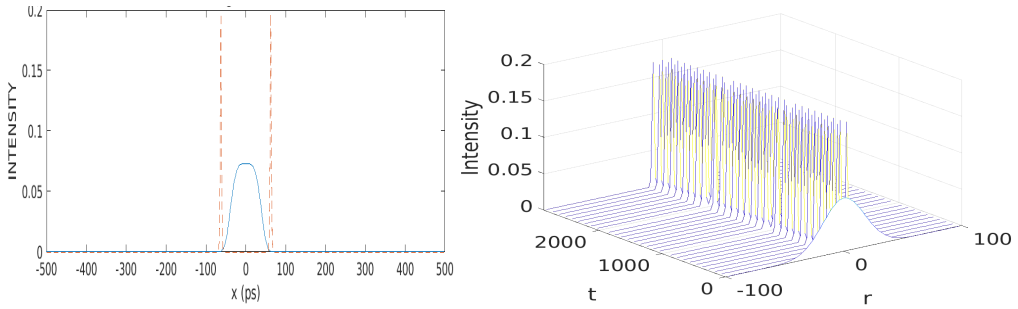

(c)

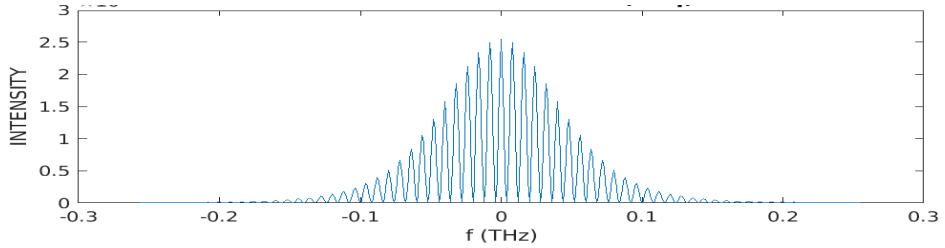

Figure 3.1.12: (a) Initial pulse is denoted by the blue line which is in the time domain and it splits into two soliton denoted by the red line. (b) 3D profile of the same. (c) Frequency comb. Here all the parameters are the same as in figure 3.1.10.

TABLE-7: Range in which we observed the frequency comb for Super Gaussian pulse where $n = 2\ and\ c = 2$.

parameters	value/range	parameters	value/range
α	3	σ	0.31,0.32
β	0.5 to 0.7	ω	1.6,1.7
s	10,10.1	θ	1.3 to 30
λ	0.5, 0.51		

If we introduce the chirping $c = 3$, we get the OFC.

(a) (b)

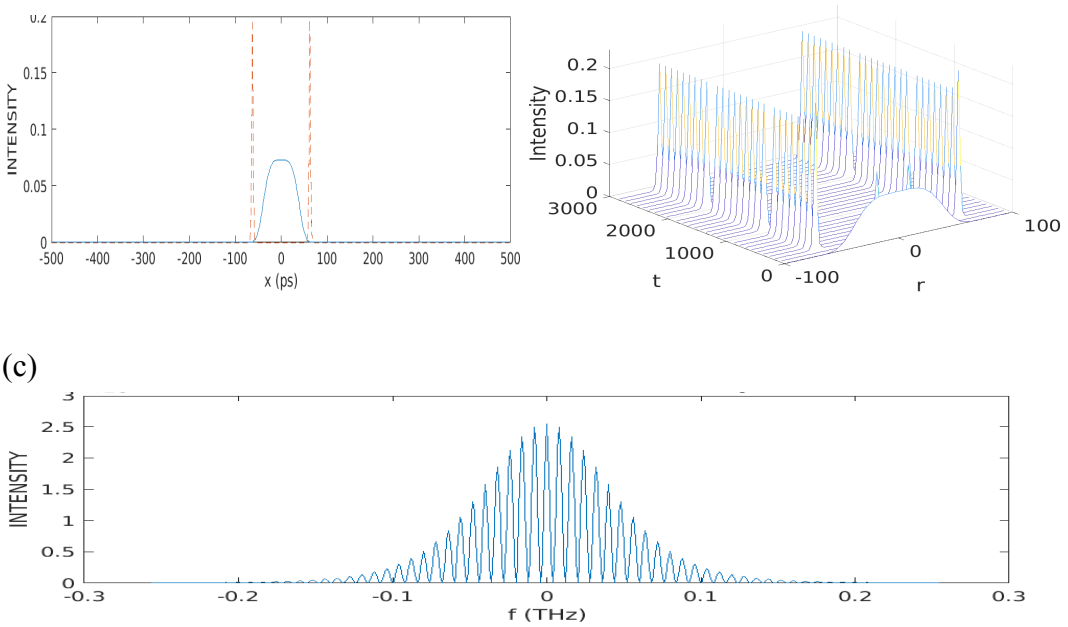

Figure 3.1.13: (a) Initial pulse is denoted by the blue line which is in the time domain and it splits into two soliton denoted by the red line. (b) 3D profile of the same. (c) Frequency comb. Here all the parameters are the same as in figure 3.1.10.

TABLE-8: Range in which we observed the frequency comb for Super Gaussian pulse where $n = 2\ and\ c = 3$.

parameters	value/range	parameters	value/range
α	3	σ	0.3,0.31
β	0.5 to 0.7	ω	1.6,1.61
s	10,10.2,10.3	θ	1.3 to 30
λ	0.5 to 0.52		

For $n = 3$, keeping all the parameters same and see the change in spectrum

(a) **(b)**

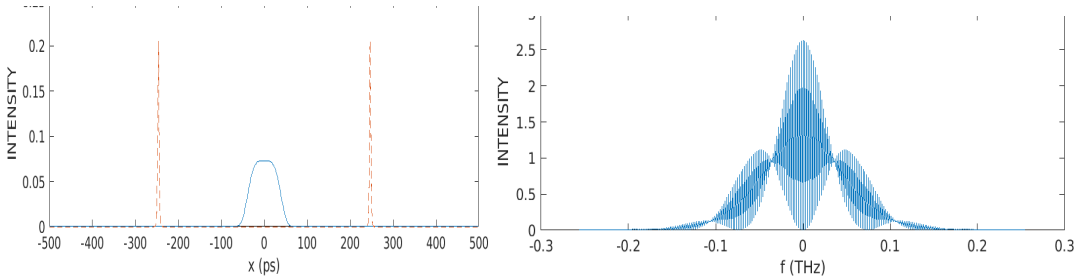

Figure 3.1.14: (a) Initial pulse is with blue line which is in the time domain and split into two cavity soliton which are in red dotted line. (b) Generation of frequency comb but not exact OFC. Here $\alpha = 2.7$, $\beta = 0.5$, $\gamma = 0.5$, $s = 10$, $\lambda = 0.5$, $\sigma = 0.3$, $\omega = 1.6$, $\theta = 1.3$.

In the above figure, we didn't get the OFC.

Now, if we change the parameter $\alpha = 2.3$.

(a) (b)

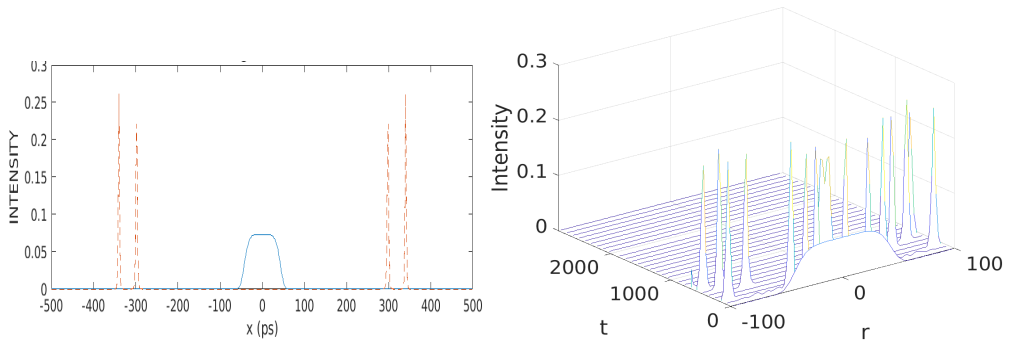

(c)

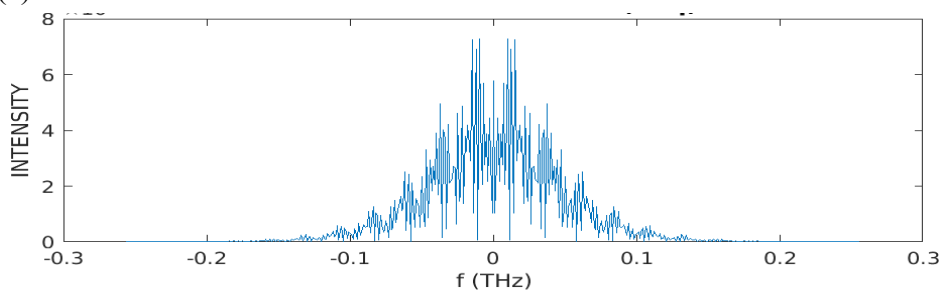

Figure 3.1.15: (a) Initial pulse is denoted by the blue line which is in the time domain and it splits into two soliton denoted by the red line. (b) 3D profile of the same. (c) Frequency comb. Here $\alpha = 2.3$and rest of the parameters are the same as in figure 3.1.14

TABLE-9: Range in which we observed the frequency comb for Super Gaussian pulse where $n = 3$.

parameters	value/range	parameters	value/range
α	2.32, 2.33, 2.35	σ	0.3
β	0.5 to 1	ω	1.6,1.8
s	9.8 to 10	θ	1.3 to 30
λ	0.5 ,0.6		

If we introduce the chirping $c = 1$and keep other parameters the same as in figure 3.1.15. we don't get the frequency comb.

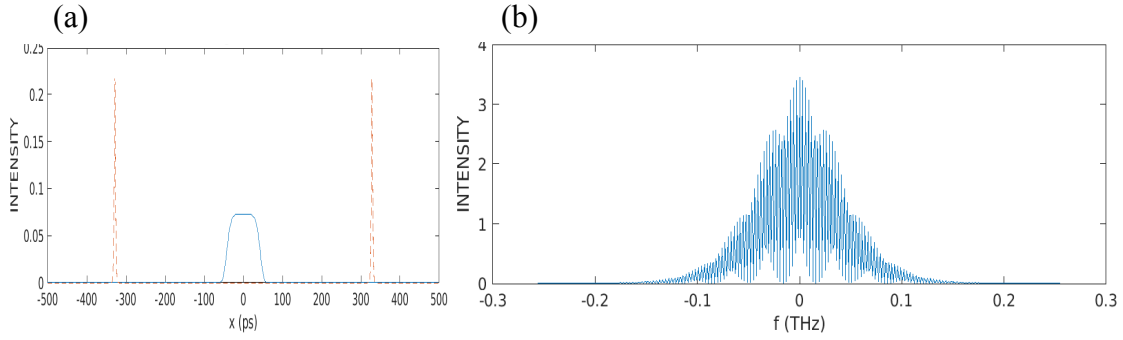

Figure 3.1.16:. (a) Initial pulse is with blue line which is in the time domain and split into two cavity soliton which are in red dotted line. (b) Generation of frequency comb but not exact OFC. Here $\alpha = 2.3,\ \beta = 0.5,\ \gamma = 0.5,\ s = 10,\ \lambda = 0.5,\ \sigma = 0.3,\ \omega = 1.6,\ \theta = 1.3$

If we change the parameter $\theta = 2$, it will give the OFC.

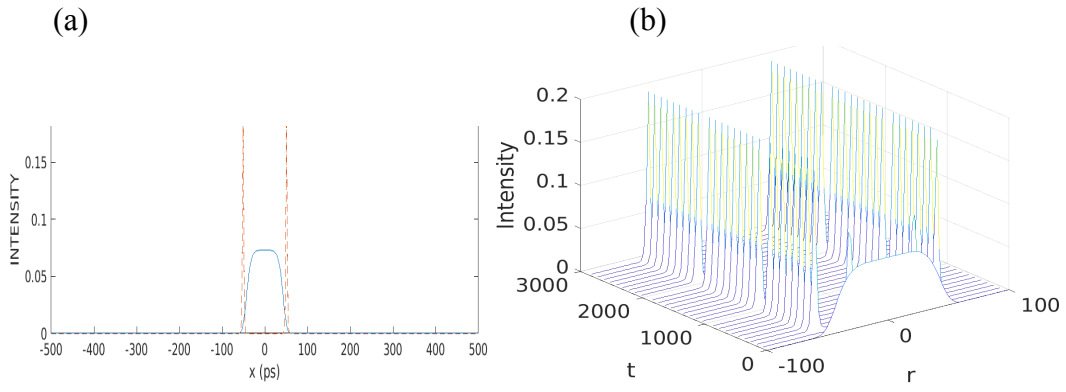

(c)

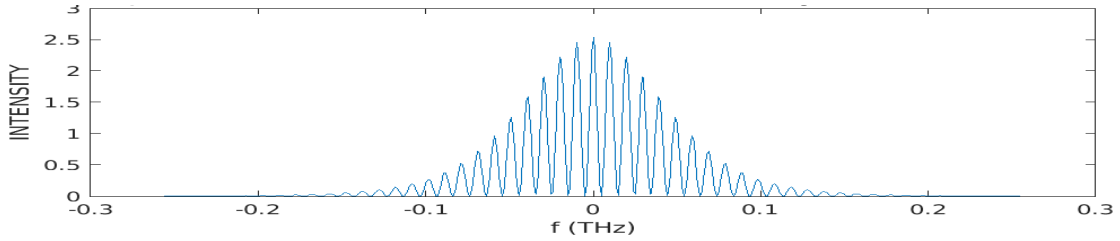

Figure 3.1.17: Initial and final pulse profile and corresponding frequency comb. (a) Blue line is the initial pulse which splits into two cavity solitons of high intensity denoted by red dotted lines. (b) Shows the initial pulse in 3D. (c) Corresponding frequency comb. Here $\theta = 2$ and the rest of the parameters are the same as in figure 3.1.16.

TABLE-10: Range in which we observed the frequency comb for Super Gaussian pulse where $n = 3\ and\ c = 1$.

parameters	value/range	parameters	value/range
α	2.3, 2.31	σ	0.3, 0.32
β	0.5, 0.8, 0.9	ω	1.6, 1.61, 1.62
s	10, 10.2 to 10.4	θ	1.3 to 30
λ	0.5 ,0.51 to 0.53		

If we introduce the chirping $c = 2$ and keeping all the parameters constant as for $c = 1$, we didn't get the OFC.

(a) (b)

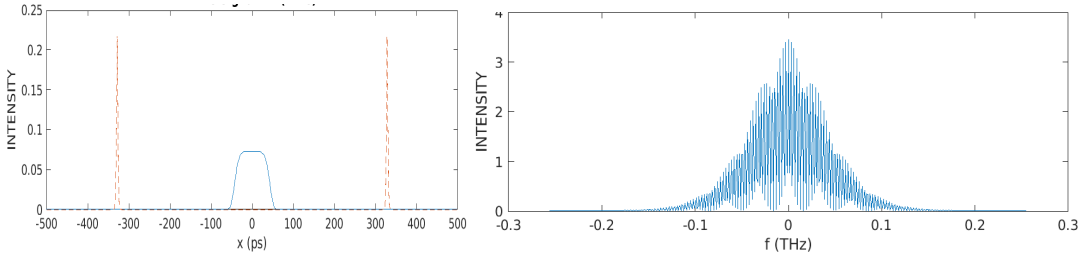

Figure 3.1.18: (a) Initial pulse is with blue line which is in the time domain and split into two cavity soliton which are in red dotted line. (b) Generation of frequency comb but not exact OFC. Here $\alpha = 2.3,\ \beta = 0.5,\ \gamma = 0.5,\ s = 10,\ \lambda = 0.5,\ \sigma = 0.3,\ \omega = 1.6,\ \theta = 1.3$

If we change the parameter alpha =2, it will give the OFC.

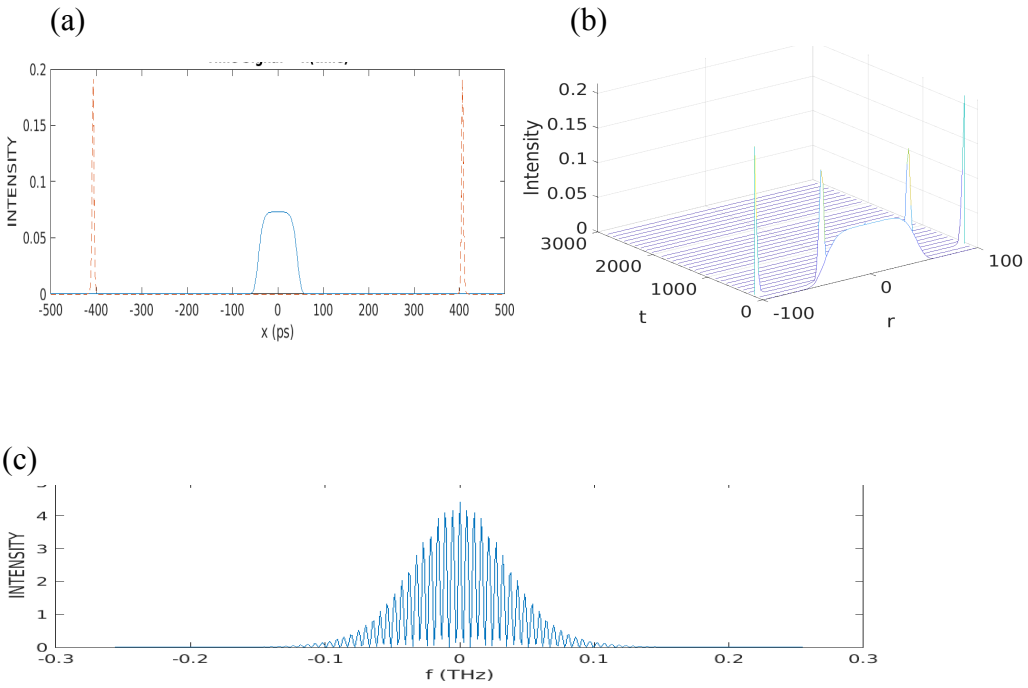

Figure 3.1.19: Initial and final pulse profile and corresponding frequency comb. (a) Blue line is the initial pulse which splits into two cavity solitons of high intensity denoted by red dotted lines. (b) Shows the initial pulse in 3D. (c) Corresponding frequency comb. Here $\alpha = 2$ and the rest of the parameters are the same as in figure 3.1.18.

TABLE-11: Range in which we found the frequency comb for Super Gaussian pulse where $n = 3\ and\ c = 2$.

parameters	value/range	parameters	value/range
α	3.2, 3.3, 3.4	σ	0.3, 0.31, 0.32
β	0.5 to 0.51 to 0.55	ω	1.6,1.8
s	10, 10.1, 10.2	θ	1.3 to 30

λ	0.5 ,0.51		

If we introduce the chirping $c = 3$, it will also not give the frequency comb.

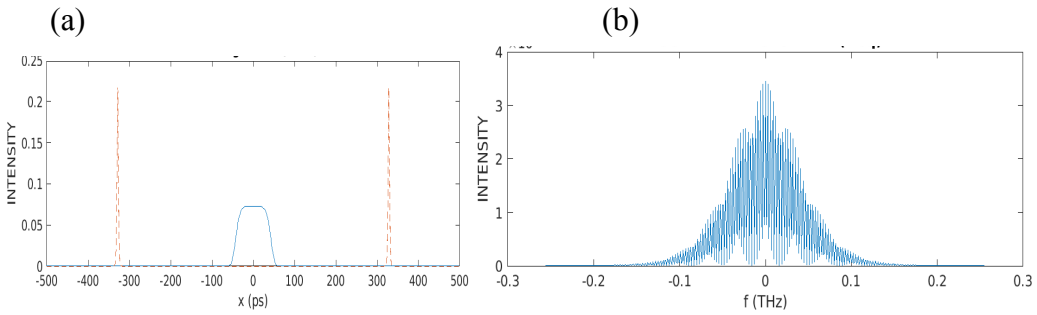

Figure3.1.20: (a) Initial pulse is with blue line which is in the time domain and split into two cavity soliton which are in red dotted line. (b) Generation of frequency comb but not exact OFC. Here $\alpha = 2.3$, $\beta = 0.5$, $\gamma = 0.5$, $s = 10$, $\lambda = 0.5$, $\sigma = 0.3$, $\omega = 1.6$, $\theta = 1.3$

If we change the parameter $\alpha = 2$,we get the OFC.

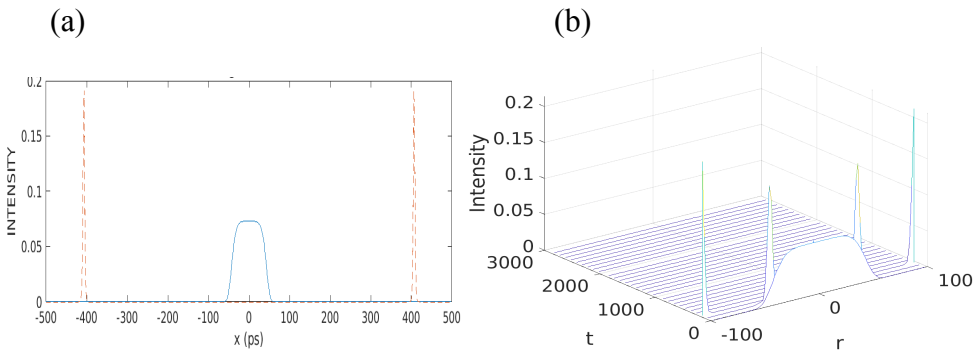

(c)

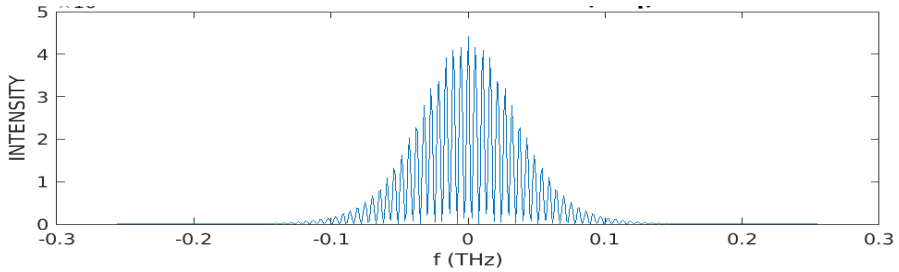

Figure 3.1.21: initial and final pulse profile and corresponding frequency comb. (a) Blue line is the initial pulse which splits into two cavity solitons of high intensity denoted by red dotted lines. (b) shows the initial pulse in 3D. (c) Corresponding frequency comb. Here $\alpha = 2$ and the rest of the parameters are the same as in figure 3.1.20.

TABLE-12: Range in which we found the frequency comb for Super Gaussian pulse where $n = 3\ and\ c = 3$.

parameters	value/range	parameters	value/range
α	2.4, 2.5, 2.6	σ	0.3,0.31
β	0.5, 0.51 to 0.55	ω	1.6,1.8
s	10, 10.1	θ	1.3 to 30
λ	0.5 ,0.51		

For $n = 4$, keeping all the parameters same as for $n = 3$ and see the change in spectrum

(a) (b)

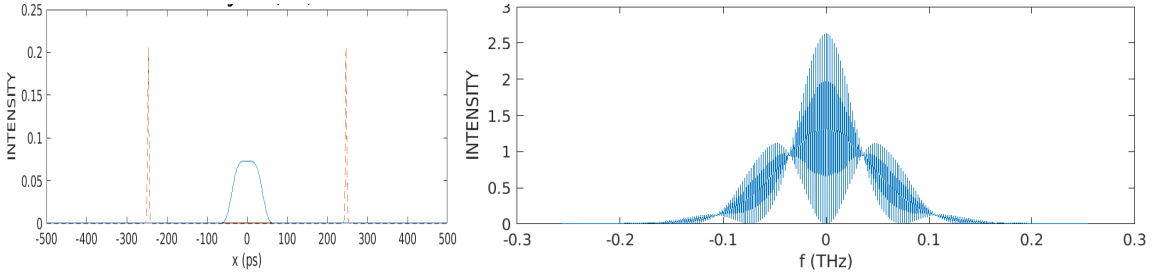

Figure 3.1.22: (a) initial pulse is with blue line which is in the time domain and split into two cavity soliton which are in red dotted line. (b) Generation of frequency comb but not exact OFC. Here $\alpha = 2.7,\ \beta = 0.5,\ \gamma = 0.5,\ s = 10,\ \lambda = 0.5,\ \sigma = 0.3,\ \omega = 1.6,\ \theta = 1.3$

In the above figure, we didn't get the OFC so to get the frequency comb we will change the parameters.

Now, if we change the parameter $\alpha = 2.8$.

(a) (b)

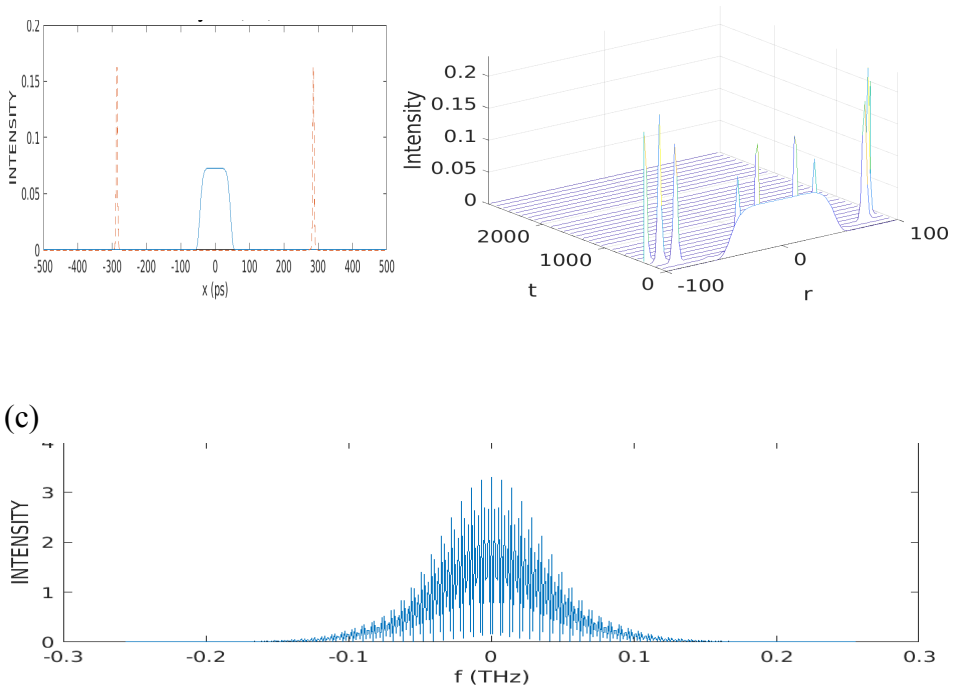

Figure3.1.23: Initial and final pulse profile and corresponding frequency comb. (a) Blue line is the initial pulse which splits into two cavity solitons of high intensity denoted by red dotted lines. (b) Shows the initial pulse in 3D. (c) Corresponding frequency comb. Here $\alpha = 2.8$ and the rest of the parameters are the same as in figure 3.1.22.

TABLE-13: Range in which we found the frequency comb for Super Gaussian pulse where $n = 4$.

parameters	value/range	parameters	value/range
α	2.8 to 3.2	σ	0.3, 0.31
β	0.5, 0.7	ω	1.6
s	10,10.1	θ	1.3 to 30
λ	0.5, 0.52, 0.53		

When we introduce the chirping $c = 1$, we will get the frequency comb.

(a) (b)

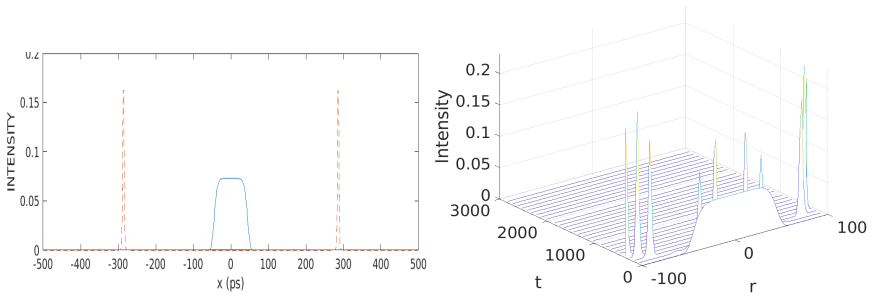

(c)

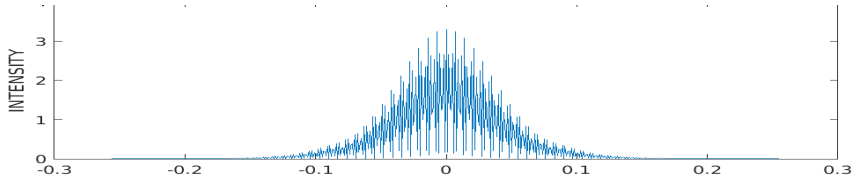

Figure 3.1.24: Initial and final pulse profile and corresponding frequency comb. (a) Blue line is the initial pulse which splits into two cavity solitons of high intensity denoted by red dotted lines. (b) Shows the initial pulse in 3D. (c) Corresponding frequency comb. Here all the parameters are the same as in figure 3.1.23.

TABLE-14: Range in which we found the frequency comb for Super Gaussian pulse where $n = 4\ and\ c = 1$.

parameters	value/range	parameters	value/range
α	2.9 to 5	σ	0.3, 0.31
β	0.5, 0.7, 0.8	ω	1.6 to 1.8
s	10, 10.1	θ	1.3 to 30
λ	0.5 to 0.52		

If we introduce the chirping $c = 2$, we get the OFC.

(a) (b)

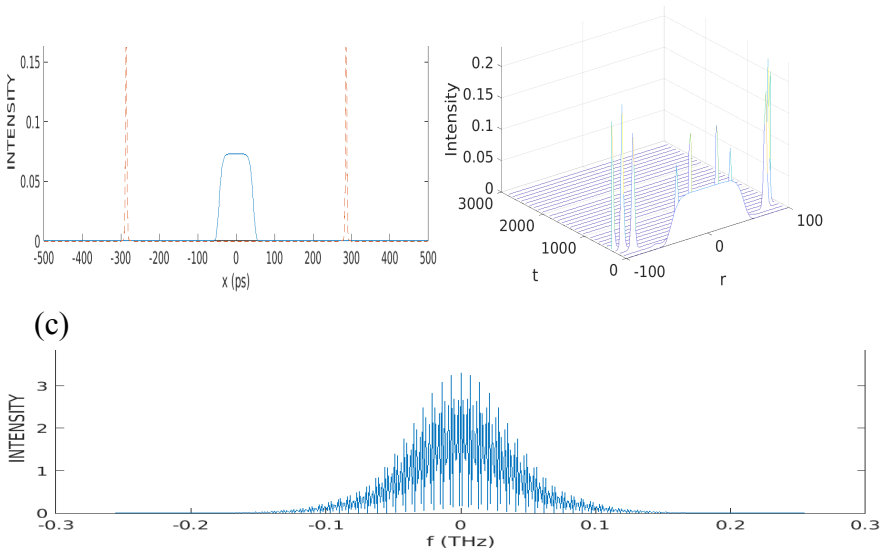

Figure 3.1.25: (a) Initial and final pulse profile and corresponding frequency comb. (a) Blue line is the initial pulse which splits into two cavity solitons of high intensity denoted by red dotted lines. (b) Shows the initial pulse in 3D. (c) Corresponding frequency comb. Here all the parameters are the same as in figure 3.1.23.

TABLE-15: Range in which we found the frequency comb for Super Gaussian pulse where $n = 4\ and\ c = 2$.

parameters	value/range	parameters	value/range
α	3.1, 3.2, 4, 5, 6	σ	0.3
β	0.5, 0.7	ω	1.6 to 1.8
s	10, 10.1	θ	1.3 to 30
λ	0.5 ,0.52, 0.53		

IF WE INTRODUCE CHIRPING $c = 3$, WE GET THE OFC

(a) (b)

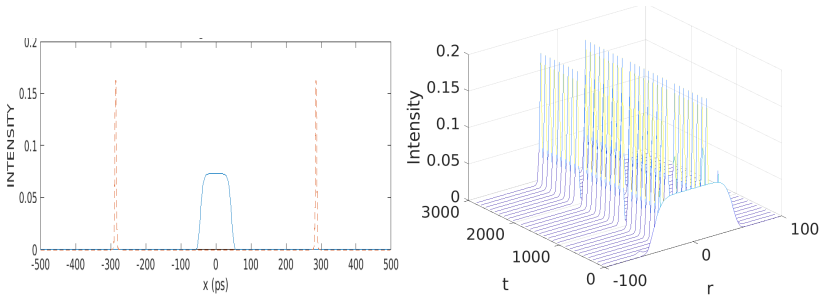

(c)

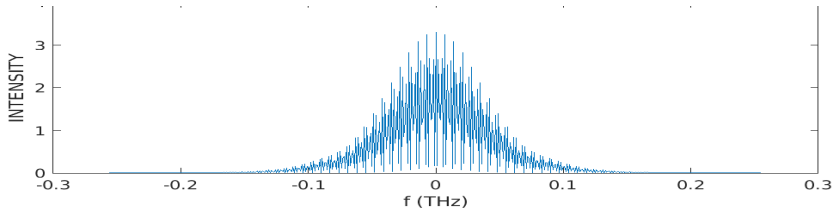

Figure 3.1.26: Initial and final pulse profile and corresponding frequency comb. (a) Blue line is the initial pulse which splits into two cavity solitons of high intensity denoted by red dotted lines. (b) Shows the initial pulse in 3D. (c) Corresponding frequency comb. Here all the parameters are the same as in figure 3.1.23.

TABLE-16: Range in which we found the frequency comb for Super Gaussian pulse where $n = 4\ and\ c = 3$.

parameters	value/range	parameters	value/range
α	3, 5, 6	σ	0.3
β	0.5, 0.7	ω	1.6
s	10, 10.1	θ	1.3 to 30
λ	0.5 ,0.52		

3. For Cosh gaussian profile i.e.,

The Cosh Gaussian profile is given by:

$$U(t) = U_0\, exp[-\frac{(t-b)^2}{2{T_0}^2}] + exp[-\frac{(t+b)^2}{2{T_0}^2}],$$

Where U_0 is maximum amplitude T is time, T_0 is half width and b is the angle

When we take the Cosh Gaussian Profile, we get the frequency comb on some particular parameters as shown in figure 3.1.27.

.

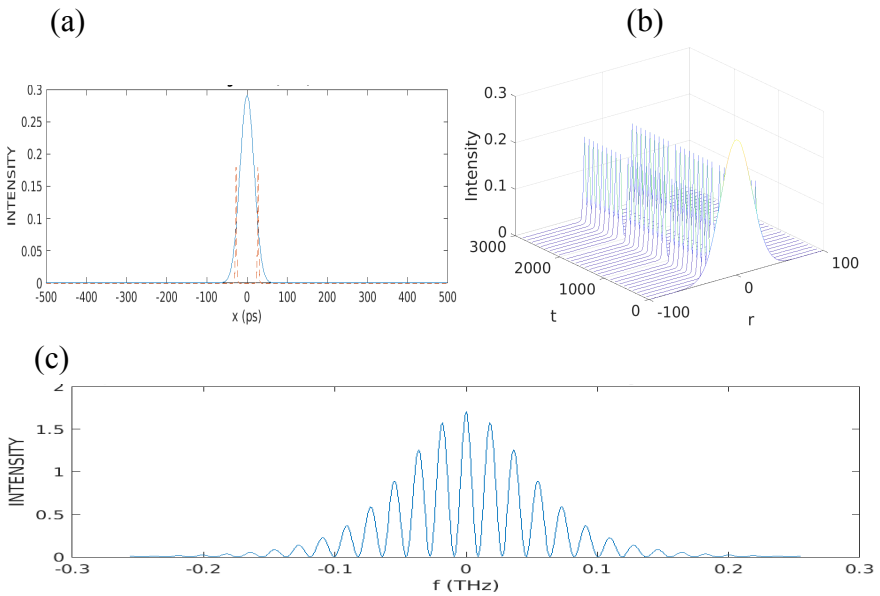

Figure 3.1.27: Initial and final pulse profile and corresponding frequency comb. (a) Blue line is the initial pulse which splits into two cavity solitons of high intensity denoted by red dotted lines. (b) Shows the initial pulse in 3D. (c) Corresponding frequency comb. Here $\alpha = 4$, $\beta = 0.5$, $\gamma = 0.5$, $s = 10$, $\sigma = 0.3$, $\omega = 1.6$, $\lambda = 0.5$and $b = 1$.

In the above figure, for $b = 1$, we get the OFC. Now we will change some other parameters and can observe the frequency comb.

WHEN $\beta = 0.6$

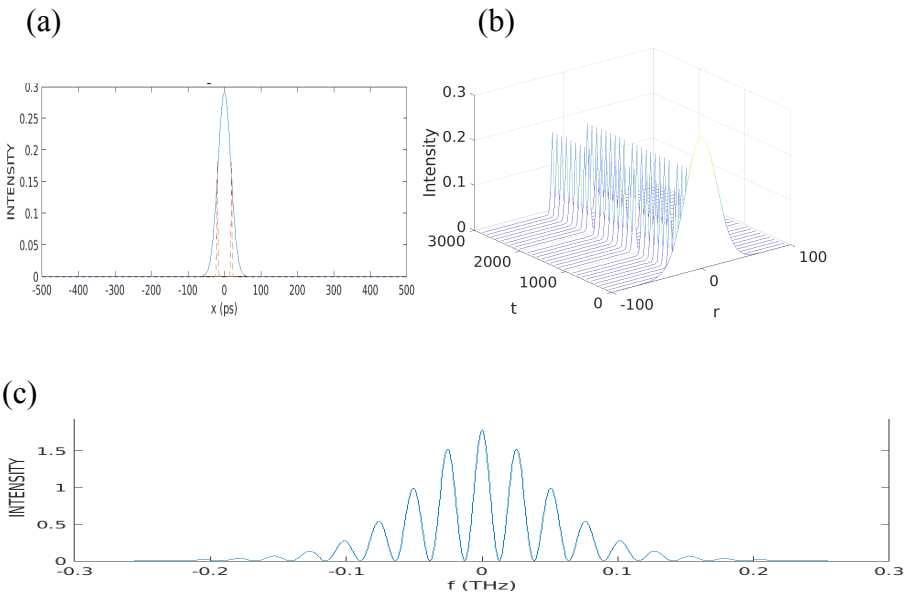

Figure 3.1.28: (a) Initial pulse is denoted by the blue line which is in the time domain and it splits into two soliton denoted by the red line. (b) 3D profile of the same. (c) Corresponding frequency comb. Here $\beta = 0.6$ and the rest of the parameters are the same as in figure 3.1.27.

TABLE-17: Range in which we get the OFC for Cosh Gaussian pulse where $b = 1$.

parameters	value/range	parameters	value/range
α	4,5	σ	0.3, 0.32, 0.33
β	0.5 to 1	ω	1.6,1.7
s	10, 10.1	θ	1.3 to 30
λ	0.52		

In the above figure 3.1.28, the initial pulse was not the cosh gaussian curve but it was the gaussian curve. The cosh gaussian curve and corresponding frequency comb will be observed by varying the different values of b.
FOR $b = 2$.

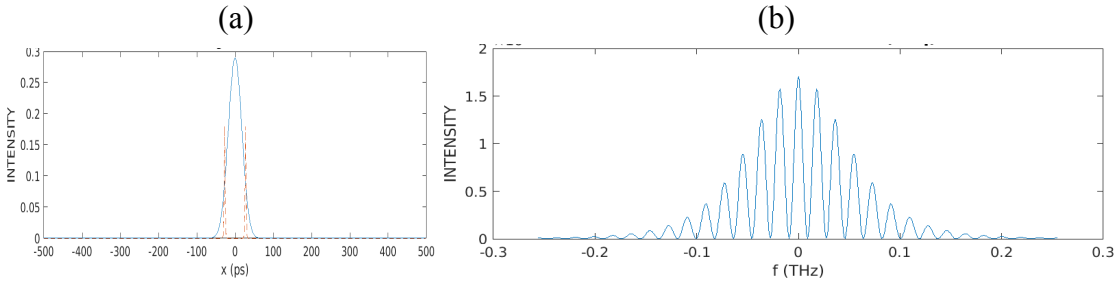

Figure 3.1.29: (a) Initial pulse is denoted by the blue line which is in the time domain and it splits into two soliton denoted by the red line. (b) Frequency comb. Here $b = 2$and all the other parameters are the same as in figure 3.1.27.

We will get the similar results for $b = 2, 3, 5\ to\ 10, 14\ to\ 19, 22, 23$.

Curve in time domain is start getting broad when $b = 25$ but don't get the exact OFC.

WHEN $b = 25$.

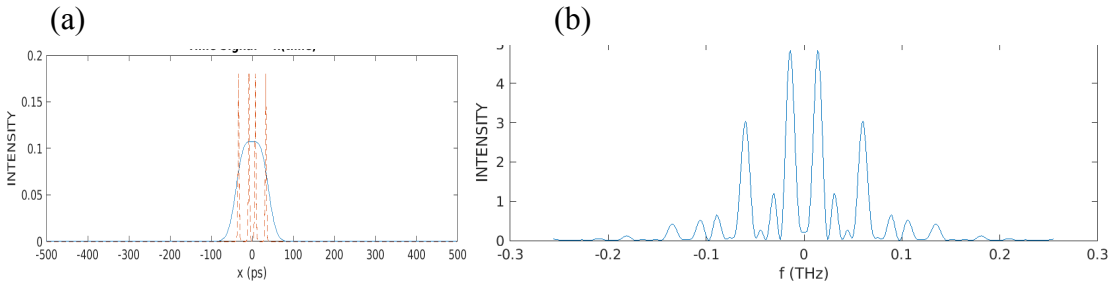

Figure 3.1.30: (a) Blue line denotes the initial pulse which is in the time domain and it splits into two soliton denoted by the red lines. (b) Generation of frequency comb but not exact OFC. Here $b = 25$and all the other parameters are the same as in figure 3.1.27.

When $b = 27$

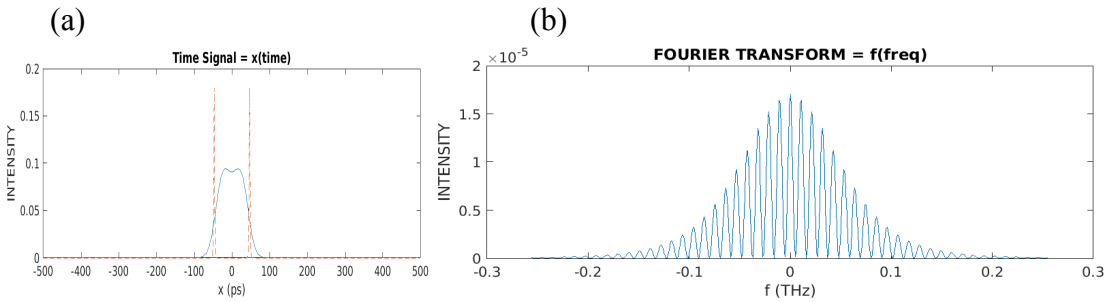

Figure 3.1.31: (a) Initial pulse is denoted by the blue line which just starts splitting in the two curves and the cavity soliton denoted by the red line. (b) Frequency comb. Here all the parameters are the same as in figure 3.1.27.

By varying the value of b from $27\ to\ 35$, we can see the curve start splitting in figure 3.1.31(a).

when$b = 45$

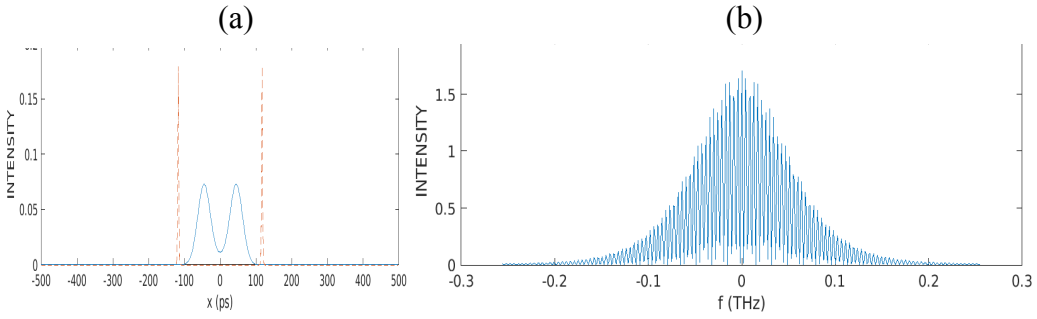

Figure 3.1.32: (a) Initial pulse is denoted by the blue line which is in the time domain and it divides into two curves and becomes a cosh gaussian pulse. Cavity solitons are denoted by the red line. (b) Frequency comb. Here $b = 45$ and the rest of the parameters are the same as in figure 3.1.27.

In the range $b = 45\ to\ 50$, we get the cosh gaussian curve as shown in figure 3.1.32(a) and corresponding frequency comb.

4. For Sinh gaussian profile i.e.,

The Sinh Gaussian profile is given by

$$U(t) = U_0\, exp[-\frac{(t-b)^2}{2{T_0}^2}] - exp[-\frac{(t+b^2)}{2{T_0}^2}],$$

Where U_0 is maximum amplitude T is time, T_0 is half width and b is the angle.

When we take the Sinh Gaussian Profile, We can observe the OFC as shown in the figure given below.

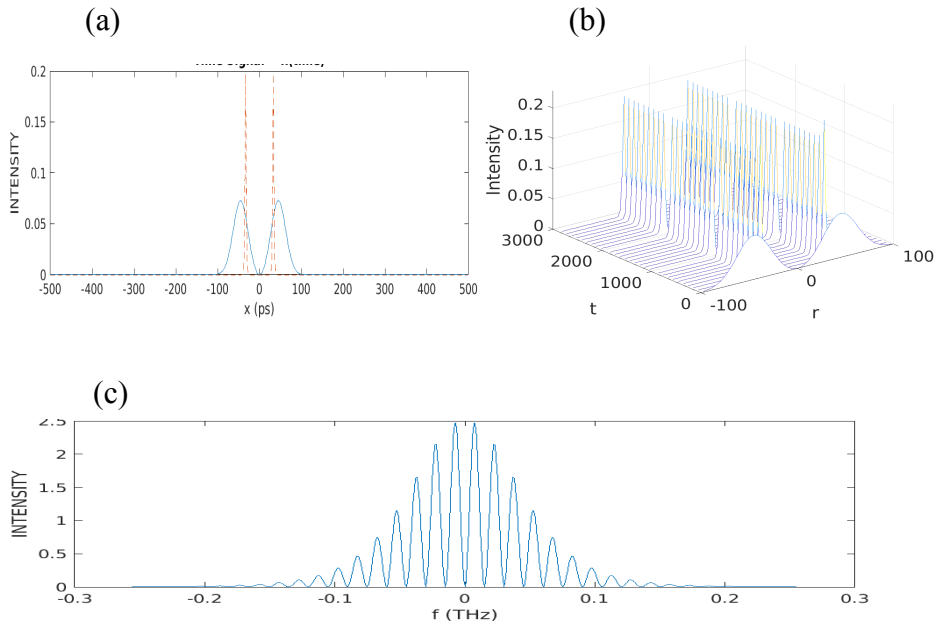

Figure3.1.33: (a) Initial pulse is denoted by the blue line which is in the time domain and it splits into two soliton denoted by the red line. (b) 3D spectrum of initial pulse (c) Frequency comb. Here $\alpha = 3,\ \beta = 0.5,\ s = 10,\ \lambda = 0.5,\ \sigma = 0.3,\ \omega = 1.6$ and $b = 45$.

TABLE-18: Range in which we found the frequency comb for Sinh Gaussian pulse is given below.

parameters	value/range	parameters	value/range

α	2, 3	σ	0.3 to 0.33
β	0.5, 0.7 to 1	ω	1.6, 1.7
s	10 to 10.6	θ	1.3 to 30
λ	0.5 to 0.53		

TABLE-19: Range in which we can find the Sinh Gaussian curve in time domain and corresponding frequency comb by varying the different values of *b* is given below.

Parameter	Range
b	20 to 22, 24, 25, 28 to 35, 37, 38, 40 to 42, 44, 45, 47 to 50

5. COMPARISON BETWEEN GAUSSIAN AND SUPER GAUSSIAN

As we see in above figures, when parameter $\beta = 0.5$, we get the frequency comb for each profile, so we will compare the number of lines/peaks by keeping the βparameter constant as 0.5.

TABLE-20:

Profile	Parameter	Number of lines
Gaussian	β=0.5	9
Super gaussian $(m = 2)$	β=0.5	49
$m = 3$	β=0.5	Didn't get the exact OFC
$m = 4$	β=0.5	47

Without chirping, we get the OFC on some particular parameters. If we keep all those parameters constant and introduce the chirping, check whether we get the OFC or not.

TABLE-21:

profile	parameter	c=1	c=2	c=3
Gaussian	α=10.1	No	No	No
Super gaussian $(m = 2)$	α=3	Yes	Yes	Yes
$m = 3$	α=2.3	No	No	No
$m = 4$	α=2.8	Yes	Yes	Yes

6. COMPARISON BETWEEN $sinh$ and $cosh$ GAUSSIAN PULSE:

TABLE-22:

profile	parameter	No. of lines
cosh	β=0.5	25
sinh	β=0.5	26

TABLE-23:

profile	Range of $b$in which the initial pulse in the time domain splits into two.
cosh	b= 45 to 50
sinh	b=20 to 50

3.2 CONCLUSION OF RESULTS:

Frequency comb has been obtained for four different input profiles, namely, Gaussian, Super-Gaussian, Cosh-Gaussian and Sinh-Gaussian. When we have the Gaussian profile, the initial pulse splits into two or more cavity solitons and we get the OFC on some particular parameters whose range is determined. When chirping is introduced by keeping all the parameters constant, we don't get the OFC but while changing the parameters, we can find the frequency comb. For the Super-Gaussian profile, when $m = 2$, the initial pulse in the time domain starts broadened and splits into two or more soliton and gives the frequency comb. When we introduce the chirping i.e., $c = 1, 2$ and 3 by keeping all the parameters constant, it will also give the frequency comb. For $m = 3$The initial pulse in the time domain expands more and gives the OFC on some particular parameters and when we introduce the

chirping, OFC will not observe so to get the frequency comb, we have to change some parameters. Similarly for $m = 4$, the initial pulse spreads more than $m = 2$ and $m = 3$, which gives the frequency comb in the frequency domain by changing some parameters. By keeping all parameters constant and introducing the chirping will also result in OFC. It can also observe if we change the parameters. We don't get the exact and perfect frequency comb for $m = 3$ as compared to $m = 2$ and $m = 4$.

For the Cosh-Gaussian profile, the initial pulse in the time domain splits into two lobes as we increase the value of 'b'. Change in 'b' by keeping the other parameters constant will result in different frequency comb.

For the cosh-Gaussian and then for Sinh-Gaussian profile, we can observe the OFC (1) by keeping 'b' constant and change other parameters and (2) by keeping other parameters constant and changing the value of 'b'.

For $\beta = 0.5$, we can find the OFC for all profiles i.e., Gaussian, Super-Gaussian, Cosh-Gaussian and Sinh-Gaussian profiles. Other parameters on which we get the OFC for each profile are $\gamma = 0.5,\ s = 10,\ \lambda = 0.5,\ \sigma = 0.3, \omega = 1.6\ and\ \theta = 1.3$.

A quick idea of the outcome of the investigation can be achieved by analysing the tables in chapter 3. The tables provide the parametric region of stable CS and more importantly stable OFC for different profiles. Further, it can be observed from the tables that by changing one or more system parameters one can tune the OFC characteristics. This is particularly helpful for experimental observation of OFC. Also this tenability may be useful for the fabrication of efficient OFC-based instruments in future.

3.3 APPLICATIONS

Main application is that – It is used to make optical atomic clocks which are hundred times more accurate as compared to other clocks and also able to improve technology of advanced communication systems. Today's best atomic clock is based on natural oscillation of cesium atoms whose frequency lies in the microwave region. So atomic clocks vibrate at microwave frequencies which have 9 billion cycles per second. That's why it oscillates much faster.

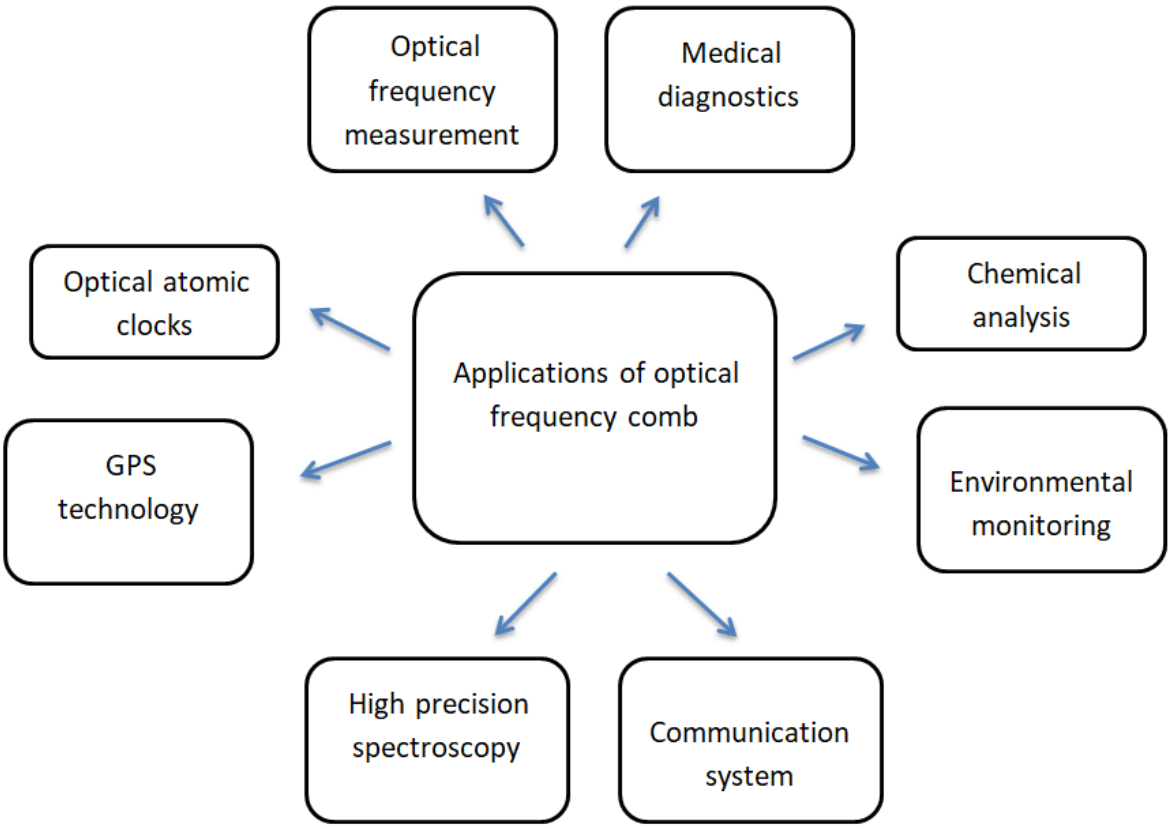

Figure 3.3.1: Show the applications of frequency comb.

3.4 FUTURE SCOPE

In the future, it may be possible that optical frequency comb generators will be developed in a compact platform to reduce the size, cost, weight and power consumption. OFC opens the new gate of optical communication, RF Processing, arbitrary wave generation and THz wireless communication. This investigation basically compares the role of different input profiles in the generation of OFC. Each profile gives different results. Also, one can identify suitable input profiles for practical use. This work can be further extended to measure the direction - To control the overall bandwidth of the OFC and the spacing between the intensity peaks. we can extend the frequency comb in the frequency domain. If the bandwidth of the OFC is in small range, it may give the result in the infrared region but for large range bandwidth, it may give the result in the ultraviolet region or in some other regions, which will be more useful and may give many other applications. OFC will be able to replace the frequency multipliers, resulting in increasing the accuracy of optical atomic clocks. Spacing between the intensity peaks indicates the time between the ultrashort pulses, which should be small so that we can get the more lines in femtoseconds.

3.5 REFERENCE

1) Paschotta, Rüdiger. "Frequency Combs.", www. rp-photonics.com.
2) Mell, Peter, and Timothy Grance. "Draft NIST working definition of cloud computing National institute of standards and technology". *Information Technology Laboratory*(2009).
3) Udem, Th, Ronald Holzwarth, and Theodor W. Hänsch. "Optical frequency metrology." *Nature* 416.6877 (2002): 233-237.
4) Cundiff, Steven T., and Jun Ye. "Colloquium: Femtosecond optical frequency combs." *Reviews of Modern Physics* 75.1 (2003): 325.
5) Ye, Jun, and Steven T. Cundiff, eds. *Femtosecond optical frequency comb: principle, operation and applications*. Springer Science & Business Media, 2005.
6) Picqué, Nathalie, and Theodor W. Hänsch. "Frequency comb spectroscopy." *Nature Photonics* 13.3 (2019): 146-157.
7) Udem, Th, Ronald Holzwarth, and Theodor W. Hänsch. "Optical frequency metrology." *Nature* 416.6877 (2002): 233-237.
8) Diddams, Scott A. "The evolving optical frequency comb." *JOSA B* 27.11 (2010): B51-B62.
9) Jones, David J., et al. "Carrier-envelope phase control of femtosecond mode-locked lasers and direct optical frequency synthesis." *Science* 288.5466 (2000): 635-639.
10) Gaeta, Alexander L., Michal Lipson, and Tobias J. Kippenberg. "Photonic-chip-based frequency combs." *Nature photonics* 13.3 (2019): 158-169.
11) Jones, David J., et al. "Carrier-envelope phase control of femtosecond mode-locked lasers and direct optical frequency synthesis." *Science* 288.5466 (2000): 635-639.
12) Lee, W., et al. ``Relative intensity noise characteristics of frequency stabilised grating-coupled mode locked semiconductor laser." *Electronics Letters* 42.20 (2006): 1156-1157.
13) Zhu, Feng, et al. "Real-time dual frequency comb spectroscopy in the near infrared." *Applied Physics Letters* 102.12 (2013): 121116.
14) Wu, Rui, et al. "Directly generated Gaussian-shaped optical frequency comb for microwave photonic filtering and picosecond pulse generation." *IEEE Photonics Technology Letters* 24.17 (2012): 1484-1486.
15) Criado, A. R., et al. "Continuous-wave sub-THz photonic generation with ultra-narrow linewidth, ultra-high resolution, full frequency range coverage and high long-term frequency stability." *IEEE Transactions on Terahertz Science and Technology* 3.4 (2013): 461-471.
16) Cundiff, Steven T., and Andrew M. Weiner. "Optical arbitrary waveform generation." *Nature Photonics* 4.11 (2010): 760-766.
17) Udem, Th, Ronald Holzwarth, and Theodor W. Hänsch. "Optical frequency metrology." *Nature* 416.6877 (2002): 233-237.
18) Giunta, Michele, et al. "20 years and 20 decimal digits: A journey with optical frequency combs." *IEEE Photonics Technology Letters* 31.23 (2019): 1898-1901.

19) Ferdous, Fahmida, et al. "Spectral line-by-line pulse shaping of on-chip microresonator frequency combs." *Nature Photonics* 5.12 (2011): 770-776.
20) Serrano, Ángel Rubén Criado, et al. "VCSEL-based optical frequency combs: Toward efficient single-device comb generation." *IEEE Photonics Technology Letters* 25.20 (2013): 1981-1984.
21) Ebeling, Karl Joachim, Rainer Michalzik, and Holger Moench. "Vertical-cavity surface-emitting laser technology applications with focus on sensors and three-dimensional imaging." *Japanese Journal of Applied Physics* 57.8S2 (2018): 08PA02.
22) Iga, Kenichi. "Vertical-cavity surface-emitting laser: Its conception and evolution." *Japanese Journal of Applied Physics* 47.1R (2008): 1.
23) Serrano, Ángel Rubén Criado, et al. "VCSEL-based optical frequency combs: Toward efficient single-device comb generation." *IEEE Photonics Technology Letters* 25.20 (2013): 1981-1984.
24) Zhou, Rui, et al. "40nm wavelength tunable gain-switched optical comb source." *Optics Express* 19.26 (2011): B415-B420.
25) Dissipative Solitons, Ed. "by N. Akhmediev and A. Ankiewicz." *Lecture Notes in Physics (Springer, Berlin* (2005).
26) Akhmediev, Nail N., and Adrian Ankiewicz. *Solitons: nonlinear pulses and beams*. Chapman & Hall, 1997.
27) Diddams, Scott A., et al. "An optical clock based on a single trapped 199Hg+ ion." *Science* 293.5531 (2001): 825-828.
28) Ackemann, Thorsten, WilliamJ Firth, and Gian‐Luca Oppo. "Fundamentals and applications of spatial dissipative solitons in photonic devices." *Advances in atomic, molecular, and optical physics* 57 (2009): 323-421.
29) Hasegawa, Akira, and Frederick Tappert. "Transmission of stationary nonlinear optical pulses in dispersive dielectric fibers. I. Anomalous dispersion." *Applied Physics Letters* 23.3 (1973): 142-144.
30) Lin, J., et al. "Short pulse generation by electrical gain switching of vertical cavity surface emitting laser." *Electronics Letters* 27.21 (1991): 1956-1958.
31) Consoli, Antonio, et al. "Characterization of Gain-Switched Pulses From 1.55-$\mu $ m VCSEL." *IEEE Photonics Technology Letters* 22.11 (2010): 772-774.
32) Supradeepa, V. R., and Andrew M. Weiner. "Bandwidth scaling and spectral flatness enhancement of optical frequency combs from phase-modulated continuous-wave lasers using cascaded four-wave mixing." *Optics letters* 37.15 (2012): 3066-3068.
33) Hammad, Mohab N., et al. "Optimum optical frequency comb generation via externally injection of a gain switched VCSEL." *CLEO: Science and Innovations*. Optical Society of America, 2019.
34) Firth, W. J., & Paulau, P. V. (2010). Soliton lasers are stabilized by coupling to a resonant linear system. *The European Physical Journal D*, *59*(1), 13-21.
35) Kaur, Baldeep, and Soumendu Jana. "Generation and dynamics of one-and two-dimensional cavity solitons in a vertical-cavity surface-emitting laser with a saturable absorber and frequency-selective feedback." *JOSA B* 34.7 (2017): 1374-1385.

36) L.A. Lugiato "Introduction to the feature section on cavity solitons: an overview," IEEE J. Quantum Elec.39, 193-196(2003).
37) Del'Haye, Pascal, et al. "Optical frequency comb generation from a monolithic microresonator." *Nature* 450.7173 (2007): 1214-1217.
38) Kourogi, Motonobu, Ken'ichi Nakagawa, and Motoichi Ohtsu. "Wide-span optical frequency comb generator for accurate optical frequency difference measurement." *IEEE Journal of Quantum Electronics* 29.10 (1993): 2693-2701.
39) Bartels, Albrecht, Dirk Heinecke, and Scott A. Diddams. "10-GHz self-referenced optical frequency comb." *Science* 326.5953 (2009): 681-681.
40) Menicucci, Nicolas C., Steven T. Flammia, and Olivier Pfister. "One-way quantum computing in the optical frequency comb." *Physical review letters* 101.13 (2008): 130501.
41) Foster, Mark A., et al. "Silicon-based monolithic optical frequency comb source." *Optics Express* 19.15 (2011): 14233-14239.
42) Del'Haye, Pascal, et al. "Full stabilization of a microresonator-based optical frequency comb." *Physical Review Letters* 101.5 (2008): 053903.
43) Bao, Hualong, et al. "Laser cavity-soliton microcombs." *Nature Photonics* 13.6 (2019): 384-389.
44) Tanguy, Y., et al. "Realization of a semiconductor-based cavity soliton laser." *Physical Review Letters* 100.1 (2008): 013907.
45) Firth, William J., et al. "Dynamical properties of two-dimensional Kerr cavity solitons." *JOSA B* 19.4 (2002): 747-752.
46) Agrawal, Govind P. "Nonlinear fiber optics." *Nonlinear Science at the Dawn of the 21st Century*. Springer, Berlin, Heidelberg, (2000): 195 - 211.
47) X.T. Tran and N.N. Rozanov, Opt. Spectrosc. 105, 432-477(2008).
48) Cundiff, Steven T., and Jun Ye. "Colloquium: Femtosecond optical frequency combs." *Reviews of Modern Physics* 75.1 (2003): 325.
49) Dissipative Solitons, Ed. "by N. Akhmediev and A. Ankiewicz." *Lecture Notes in Physics (Springer, Berlin* (2005).
50) Biswas, Anjan. "Theory of optical couplers." *Optical and quantum electronics* 35.3 (2003): 221-235.
51) Miller, Jonah Maxwell. "Optimizing and applying graphene as a saturable absorber for generating ultrashort pulses." (2011).
52) JOHNSON, RALPH, ANDREW CLARK, and JAMES GUNTER. "Coupled cavity Anti-guided vertical cavity surface emitting laser (VCSEL)." (2001).
53) Ebeling, Karl Joachim, Rainer Michalzik, and Holger Moench. "Vertical-cavity surface-emitting laser technology applications with focus on sensors and three-dimensional imaging." *Japanese Journal of Applied Physics* 57.8S2 (2018): 08PA02.
54) J. M. Miller et al. A systematic study of techniques to directly measure the saturable absorption of graphene. In Annual Meeting of the Four Corners Section of the American Physical Society, volume 55, 2010.
55) Taylor, Luke. "A comparison between the Split Step Fourier and Finite-Difference method in analysing the soliton collision of a type of Nonlinear Schr\" odinger

equation found in the context of optical pulses." *arXiv preprint arXiv:1709.04805* (2017).

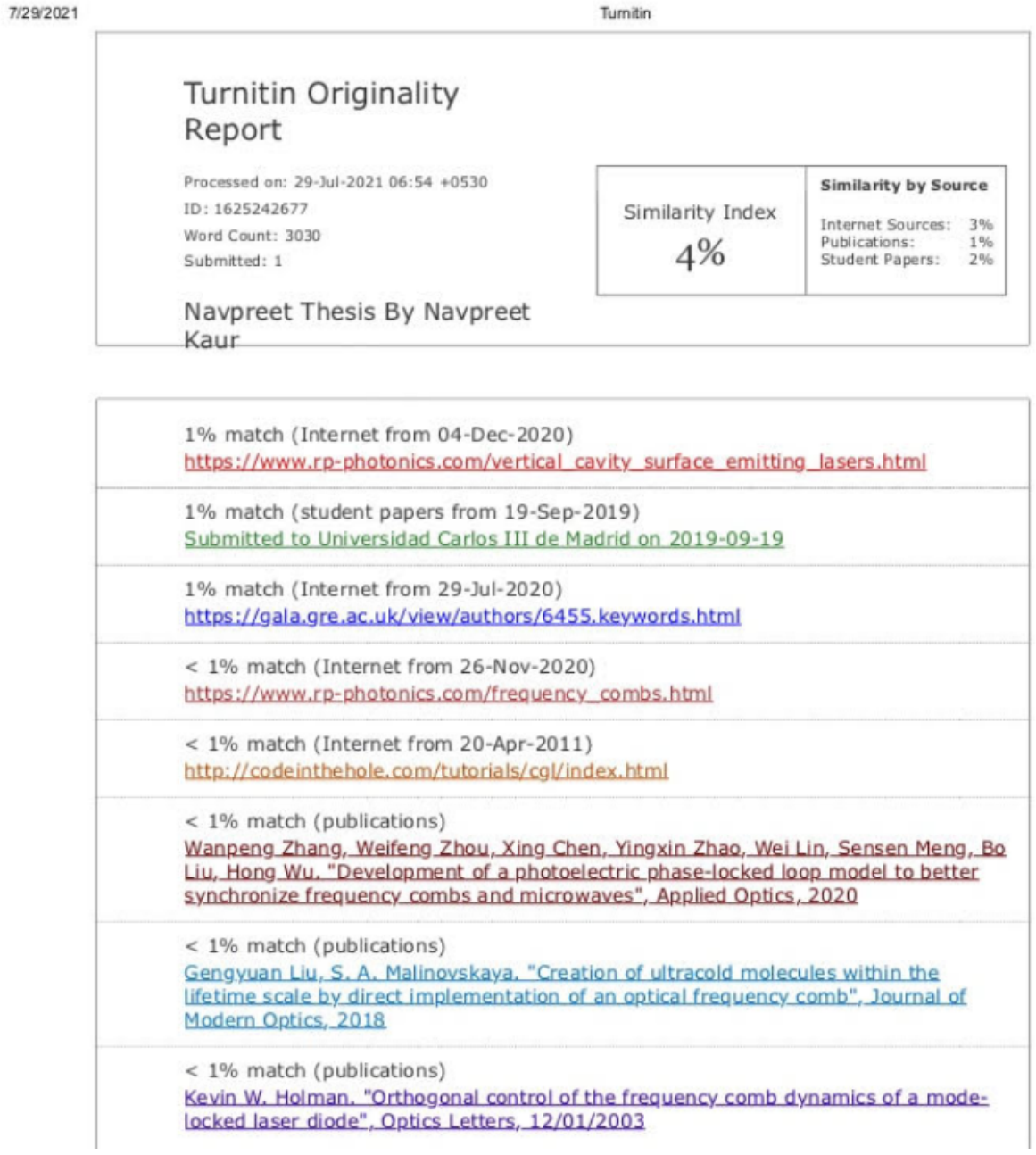

7/29/2021 Turnitin

Turnitin Originality Report

Processed on: 29-Jul-2021 06:54 +0530
ID: 1625242677
Word Count: 3030
Submitted: 1

Navpreet Thesis By Navpreet Kaur

Similarity Index	Similarity by Source	
4%	Internet Sources:	3%
	Publications:	1%
	Student Papers:	2%

1% match (Internet from 04-Dec-2020)
https://www.rp-photonics.com/vertical_cavity_surface_emitting_lasers.html

1% match (student papers from 19-Sep-2019)
Submitted to Universidad Carlos III de Madrid on 2019-09-19

1% match (Internet from 29-Jul-2020)
https://gala.gre.ac.uk/view/authors/6455.keywords.html

< 1% match (Internet from 26-Nov-2020)
https://www.rp-photonics.com/frequency_combs.html

< 1% match (Internet from 20-Apr-2011)
http://codeinthehole.com/tutorials/cgl/index.html

< 1% match (publications)
Wanpeng Zhang, Weifeng Zhou, Xing Chen, Yingxin Zhao, Wei Lin, Sensen Meng, Bo Liu, Hong Wu. "Development of a photoelectric phase-locked loop model to better synchronize frequency combs and microwaves", Applied Optics, 2020

< 1% match (publications)
Gengyuan Liu, S. A. Malinovskaya. "Creation of ultracold molecules within the lifetime scale by direct implementation of an optical frequency comb", Journal of Modern Optics, 2018

< 1% match (publications)
Kevin W. Holman. "Orthogonal control of the frequency comb dynamics of a mode-locked laser diode", Optics Letters, 12/01/2003